Electronic Journal of Applied Statistical Analysis
EJASA, Electron. J. App. Stat. Anal.
`http://siba-ese.unisalento.it/index.php/ejasa/index`
e-ISSN: 2070-5948
DOI: 10.1285/i20705948v17n3p676

A New Generalized Gamma Type II Exponentiated Half Logistic-Topp-Leone-G Family of Distributions with Applications

By Charumbira, Oluyede, Chipepa

15 December 2024

Electronic Journal of Applied Statistical Analysis
Vol. 17, Issue 03, December 2024, 676-702
DOI: 10.1285/i20705948v17n3p676

A New Generalized Gamma Type II Exponentiated Half Logistic-Topp-Leone-G Family of Distributions with Applications

Wellington Fredrick Charumbira*[ab], Broderick Oluyede[a], and Fastel Chipepa[a]

[a] *Botswana International University of Science and Technology, Department of Mathematics and Statistical Sciences, P. Bag 16, Palapye, Botswana*
[b] *Midlands State University, Department of Applied Mathematics and Statistics, P. Bag 9055 Gweru, Zimbabwe*

15 December 2024

In this research, we introduce a novel family of distributions titled the Gamma Type II Exponentiated Half Logistic-Topp-Leone-G (RB-TII-EHL-TL-G) distribution. The series expansion, order statistics, uncertainty measures, stochastic orders and moments are some of the mathematical and statistical properties that were derived. We estimated the parameters using various techniques including least squares (LS), maximum likelihood (ML), Anderson-Darling (AD), and Cramér-von-Mises (CVM). Based on the Monte Carlo simulation results, the ML estimation method demonstrated superior performance compared to other estimation techniques examined, leading to its selection for estimating the model parameters. By fitting the Gamma Type II Exponentiated Half Logistic-Topp-Leone-Weibull (RB-TII-EHL-TL-W) distribution, a special case of the RB-TII-EHL-TL-G family to two real-world data sets from different fields, we demonstrate its superiority over nested and non-nested models.

keywords: Maximum Likelihood, Gamma Generator, Topp-Leone Distribution, Exponentiated Half Logistic Distribution, Stochastic Orders, Monte Carlo Simulation.

*Corresponding authors: cw22100040@studentmail.biust.ac.bw

ISSN: 2070-5948
http://siba-ese.unisalento.it/index.php/ejasa/index

1 Introduction

Statistical distributions serve as powerful tools for explaining diverse real-life events, enabling us to uncover underlying patterns, trends and behaviors of data. Researchers have been motivated to extend classical distributions so as to come up with flexible distributions that can better accommodate various data fitting requirements. This drive arises from the limitations in most standard distributions such as logistic, Lindley, gamma, exponential, and Burr XII distributions. Some notable examples of new generalizations with wide applications include the Topp-Leone-Marshall-Olkin-G family of distributions (Chipepa et al., 2020), odd Weibull Topp-Leone-G power series class of distributions (Oluyede et al., 2021), Marshall Olkin Pranav distribution (Alsultan, 2023), odd power generalized Weibull-G power series class of distributions (Oluyede et al., 2022a) and the Topp-Leone-Harris-G family of distributions (Oluyede et al., 2023) among others. These extensions provide versatile and adaptable models with diverse applications.

The gamma transformation has emerged as a valuable tool for extending and enriching a wide range of distributions available literature. By leveraging the flexibility and versatility of the gamma transformation, researchers have been able to generate novel distributions that offer unique characteristics and broader applicability. These new distributions provide valuable alternatives for modeling various real-life phenomena and addressing specific modeling challenges. The following are recent distributions generated by the gamma transformation: gamma odd power generalized Weibull-G family of distributions (Gabanakgosi et al., 2021), gamma odd Burr III-G family of distributions (Peter et al., 2021) and the gamma Topp-Leone type II exponentiated half logistic Weibull distribution (Oluyede et al., 2023).

Different methods of estimation are essential in developing new generalized distributions, as each approach offers unique strengths for parameter estimation. For instance, the maximum likelihood estimation provides efficient and consistent estimates, particularly beneficial for large samples. The least squares technique minimizes the sum of the squared differences between observed and predicted values, ensuring a close fit to the data. Evaluating the best method for estimating parameters in a new family of distributions is crucial, especially for the applications of the model. For further insights into various estimation methods, refer to Dey et al. (2015), Ali et al. (2021), and Warahena-Liyanage et al. (2023) among others.

The Topp-Leone distribution (Topp and Leone, 1955) is a bounded distribution with domain between 0 and 1, and possesses a J-shaped probability density function, hence it is not flexible. However, its subsequent extensions have exhibited greater flexibility.

Moakofi et al. (2021) developed the type II exponentiated half logistic-Topp-Leone-G (TII-EHL-TL-G) family of distributions with cumulative distribution function (cdf)

$$F_{TII-EHL-TL}(z;\alpha,\vartheta,\underline{\zeta}) \quad = \quad 1 - W_G(z;\alpha,\vartheta,\underline{\zeta}) \tag{1}$$

and probability density function (pdf)

$$\begin{aligned} f_{TII-EHL-TL}(z;\alpha,\vartheta,\underline{\zeta}) &= 4\alpha\vartheta g(z;\underline{\zeta})[1-\bar{G}^2(z;\underline{\zeta})]^{\vartheta-1}\bar{G}(z;\underline{\zeta}) \\ &\times \frac{\left(1-[1-\bar{G}^2(z;\underline{\zeta})]^{\vartheta}\right)^{\alpha-1}}{\left(1+[1-\bar{G}^2(z;\underline{\zeta})]^{\vartheta}\right)^{\alpha+1}}, \end{aligned} \tag{2}$$

for $\alpha,\vartheta > 0$, where $W_G(z;\alpha,\vartheta,\underline{\zeta}) = \left[\frac{1-[1-\bar{G}^2(z;\underline{\zeta})]^{\vartheta}}{1+[1-\bar{G}^2(z;\underline{\zeta})]^{\vartheta}}\right]^{\alpha}$ and $\underline{\zeta}$ is the parent parameter vector.

The gamma generator has cdf

$$\begin{aligned} F_{RB}(z;\sigma,\underline{\zeta}) &= 1-\frac{1}{\Gamma(\sigma)}\int_0^{-\log[G(z;\underline{\zeta})]} t^{\sigma-1}e^{-t}dt \\ &= 1-\frac{\gamma(\sigma,-\log[G(z;\underline{\zeta})])}{\Gamma(\sigma)}. \end{aligned} \tag{3}$$

and pdf

$$f_{RB}(z;\sigma,\underline{\zeta}) = \frac{1}{\Gamma(\sigma)}(-\log[G(z;\underline{\zeta})])^{\sigma-1}g(z;\underline{\zeta}), \tag{4}$$

for $\sigma > 0$, and parent parameter vector $\underline{\zeta}$ (Ristić and Balakrishnan, 2012).

The motivations for introducing the RB-TII-EHL-TL-G family of distributions include:

- Addressing limitations of earlier families: The new family of distributions addresses the shortcomings of the Topp-Leone-G and TII-EHL-G families. It provides improved tail behavior and increased flexibility through the incorporation of an additional shape parameter σ. This improvement allows for more effective modeling of complex data patterns and provides better data fitting compared to some of its nested models.

- Flexibility in data fitting: The RB-TII-EHL-TL-G family of distributions offers enhanced flexibility for accurately fitting various types of data. It can effectively handle datasets with both monotonic and non-monotonic hazard rate functions.

- Comparison of estimation methods: Comparing different estimation techniques via Monte Carlo simulations helps to identify the best method for estimating the parameters of the RB-TII-EHL-TL-G family of distributions. This helps to ensure accurate parameter estimation and reliable inference.

- Wide applicability: The RB-TII-EHL-TL-G family of distributions finds applications in diverse fields like biology, finance, physics, and economics. Its versatility makes it a valuable tool for analyzing data in various domains.

Structure of the paper: The new family of distributions, its subfamilies, series expansion and representation and the quantile function are presented in Section 2. Section 3 contains a selection of the new family's special cases. Section 4 consists of additional statistical properties of the new family of distributions including order statistics, uncertainty measure, moments and stochastic orders. Section 5 focuses on various estimation techniques for the new family of distributions while Section 6 dwells on the Monte Carlo simulations. Section 7 showcases applications of the RB-TIIEHL-TL-W distribution a special case of the RB-TII-EHL-TL-G family of distributions to real-world data. Section 8 presents a summary of the main findings and conclusions drawn from the study.

2 The New Family and Statistical Properties

Section 2 introduces the new RB-TII-EHL-TL-G family of distributions, along with its subfamilies and some statistical properties, including the quantile function and series expansion and representation.

2.1 The New Family

Taking Equation (1) to be the parent cdf of Equation (3), we get the RB-TII-EHL-TL-G family of distributions with cdf

$$\begin{aligned} F(z;\sigma,\alpha,\vartheta,\underline{\zeta}) &= 1-\frac{1}{\Gamma(\sigma)}\int_0^{-\log\left[1-W_G(z;\alpha,\vartheta,\underline{\zeta})\right]} t^{\sigma-1}e^{-t}dt \\ &= 1-\frac{\gamma\left(\sigma,-\log\left[1-W_G(z;\alpha,\vartheta,\underline{\zeta})\right]\right)}{\Gamma(\sigma)}, \end{aligned} \tag{5}$$

and pdf

$$\begin{aligned} f(z;\sigma,\alpha,\vartheta,\underline{\zeta}) &= \frac{4\alpha\vartheta}{\Gamma(\sigma)}\left(-\log\left[1-W_G(z;\alpha,\vartheta,\underline{\zeta})\right]\right)^{\sigma-1} g(z;\underline{\zeta}) \\ &\times \frac{[1-\bar{G}^2(z;\underline{\zeta})]^{\vartheta-1}\bar{G}(z;\underline{\zeta})\left(1-[1-\bar{G}^2(z;\underline{\zeta})]^{\vartheta}\right)^{\alpha-1}}{(1+[1-\bar{G}^2(z;\underline{\zeta})]^{\vartheta})^{\alpha+1}}, \end{aligned} \tag{6}$$

for $\sigma,\alpha,\vartheta>0$ and parent parameter vector $\underline{\zeta}$.

2.2 Sub-Families

We present sub-familes of the RB-TII-EHL-TL-G family of distributions in this subsection.

- If $\sigma=1$, we get the TII-EHL-TL-G family of distributions with cdf

$$F(z;\alpha,\vartheta,\underline{\zeta}) = 1-W_G(z;\alpha,\vartheta,\underline{\zeta}),$$

  for $\alpha,\vartheta>0$, and $\underline{\zeta}$ is the parent parameter vector (Moakofi et al., 2021).

- If we set $\alpha = 1$, we get a reduced family of distributions with cdf

$$F(z;\sigma,\vartheta,\underline{\zeta}) \;=\; 1 - \frac{\gamma\left(\sigma, -\log\left[1-\left[\frac{1-[1-\bar{G}^2(z;\underline{\zeta})]^{\vartheta}}{1+[1-\bar{G}^2(z;\underline{\zeta})]^{\vartheta}}\right]\right]\right)}{\Gamma(\sigma)},$$

for $\vartheta, \sigma > 0$, and parent parameter vector $\underline{\zeta}$.

- If $\vartheta = 1$, we get a reduced family with cdf

$$F(z;\sigma,\alpha,\underline{\zeta}) \;=\; 1 - \frac{\gamma\left(\sigma, -\log\left[1-\left[\frac{1-[1-\bar{G}^2(z;\underline{\zeta})]}{1+[1-\bar{G}^2(z;\underline{\zeta})]}\right]^{\alpha}\right]\right)}{\Gamma(\sigma)},$$

for $\alpha, \sigma > 0$, and parent parameter vector $\underline{\zeta}$.

- If $\alpha = \vartheta = 1$, we get a reduced family with cdf

$$F(z;\sigma,\underline{\zeta}) \;=\; 1 - \frac{\gamma\left(\sigma, -\log\left[1-\left[\frac{1-[1-\bar{G}^2(z;\underline{\zeta})]}{1+[1-\bar{G}^2(z;\underline{\zeta})]}\right]\right]\right)}{\Gamma(\sigma)},$$

for $\sigma > 0$, and parent parameter vector $\underline{\zeta}$.

- If $\alpha = \sigma = 1$, we get a new family of distributions with cdf

$$F(z;b,\underline{\zeta}) \;=\; 1 - \left[\frac{1-[1-\bar{G}^2(z;\underline{\zeta})]^{\vartheta}}{1+[1-\bar{G}^2(z;\underline{\zeta})]^{\vartheta}}\right],$$

for $\vartheta > 0$, and parent parameter vector $\underline{\zeta}$.

- If $\alpha = \vartheta = \sigma = 1$, we get a new family of distributions with cdf

$$F(z;\underline{\zeta}) \;=\; 1 - \left[\frac{1-[1-\bar{G}^2(z;\underline{\zeta})]}{1+[1-\bar{G}^2(z;\underline{\zeta})]}\right],$$

where $\underline{\zeta}$ is the parent parameter vector.

2.3 Quantile Function

The quantile function is a fundamental statistical tool with a wide range of applications. It can be used to generate random numbers, compute extreme quantiles and evaluate skewness and kurtosis. The RB-TII-EHL-TL-G family of distribution's quantile function is

$$Q_Z(p) = G^{-1}\left(1-\left[1-\left[\frac{1-\left(1-\exp\{\gamma^{-1}[\sigma,\Gamma(\sigma)(1-p)]\}\right)^{\frac{1}{\alpha}}}{1+\left(1-\exp\{\gamma^{-1}[\sigma,\Gamma(\sigma)(1-p)]\}\right)^{\frac{1}{\alpha}}}\right]^{\frac{1}{\vartheta}}\right]^{0.5}\right),$$

for $\sigma, \alpha, \vartheta > 0$, where $0 \le p \le 1$ and G is the parent distribution.

2.4 Series Expansion and Representation

This subsection presents the expansion of the density of our proposed model. We can express the RB-TII-EHL-TL-G pdf as

$$f(z;\sigma,\alpha,\vartheta,\underline{\zeta}) = \sum_{p=0}^{\infty} \eta_{p+1} g_{p+1}(z;\underline{\zeta}), \tag{7}$$

where

$$\begin{aligned} \eta_{p+1} &= \frac{4\alpha\vartheta}{\Gamma(\sigma)} \sum_{m,s,j,k,l=0}^{\infty} (-1)^{j+l+m} b_{s,m} \binom{\sigma-1}{m} \binom{\alpha(m+s+\sigma)-1}{j} \\ &\times \binom{-\alpha(m+s+\sigma)-1}{k} \binom{\vartheta(j+k+1)-1}{l} \binom{2l+1}{p} \left(\frac{1}{p+1}\right), \end{aligned} \tag{8}$$

and $g_{p+1}(z;\underline{\zeta}) = (p+1)G^p(z;\underline{\zeta})g(z;\underline{\zeta})$ is the exponentiated-G (Expo-G) pdf with parameter $(p+1)$. Equation (7) and the accompanying properties of the Expo-G distribution make it possible to obtain the various mathematical properties of our proposed family of distributions. *For derivations, please refer to the Web Appendix.*

3 Special Cases

In this part we provide two special cases of the RB-TII-EHL-TL-G family of distributions.

Table 1: Special Cases

Baseline	Special Case
Weibull(W)	Gamma-Type II Exponentiated Half Logistic-Topp-Leone-Weibull (RB-TII-EHL-TL-W)
Log-logistic(LLoG)	Gamma-Type II Exponentiated Half Logistic-Topp-Leone-Log-logistic (RB-TII-EHL-TL-LLoG)

Table 1 presents special cases for the RB-TII-EHL-TL-G family of distributions.

3.1 RB-TII-EHL-TL-W Distribution

Graphs of the pdfs (Figure 1) show several shapes including left-skewed, reverse-J, right-skewed and almost symmetric shapes. The graphs of hrfs illustrate bathtub, inverted bathtub, increasing and decreasing patterns.

Figure 2 displays 3D graphs illustrating the skewness and kurtosis of the RB-TL-TII-EHL-W distribution. The graphs show that if we fix α and σ, both skewness and and kurtosis are high for low values of ϑ and λ. This is an indication of pronounced asymmetry and heavy tails. Conversely, as ϑ and λ increase, both skewness and kurtosis decrease, suggesting that the distribution approaches a more symmetrical and light-tailed form.

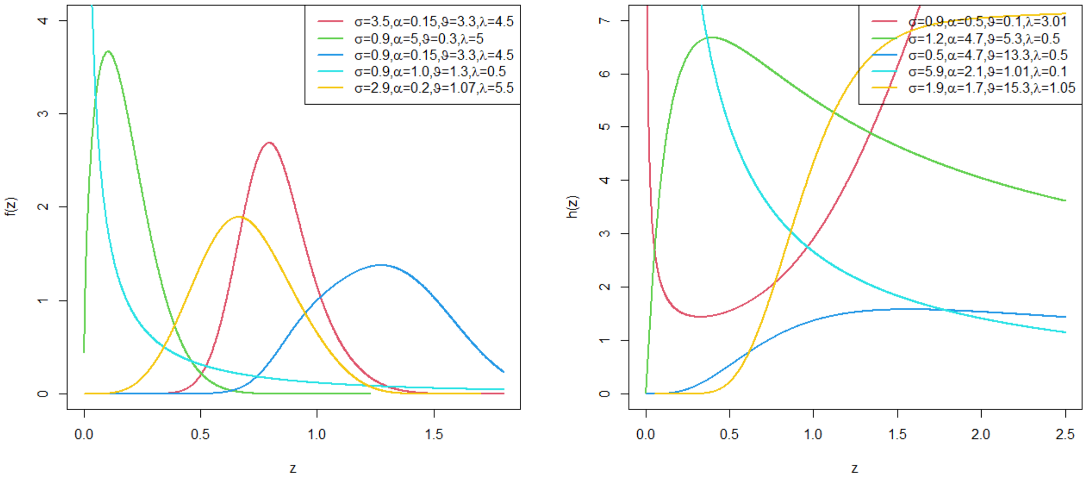

Figure 1: RB-TII-EHL-TL-W pdf and hrf plots

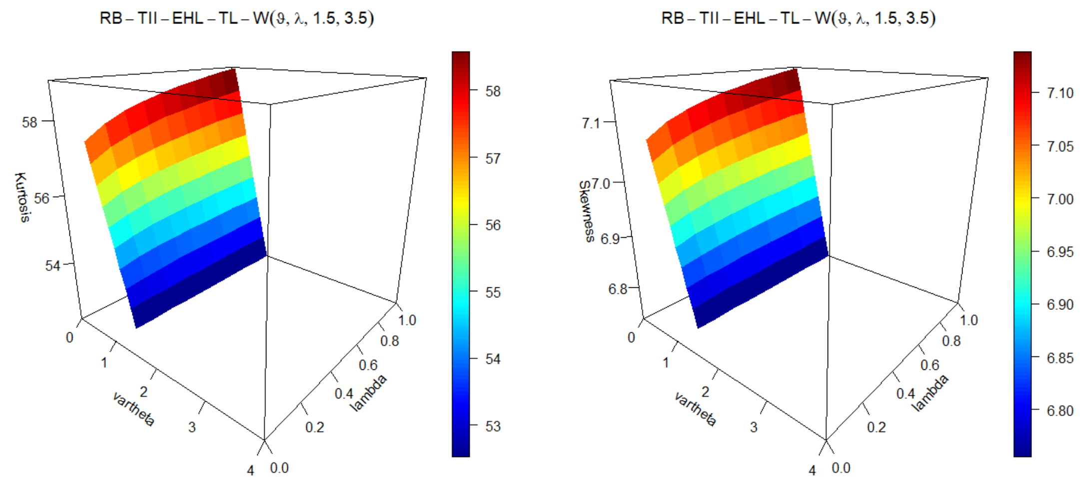

Figure 2: 3D Graphs of the RB-TL-TII-EHL-W Skewness and Kurtosis

3.2 RB-TII-EHL-TL-LLoG Distribution

Plots of the pdf on Figure 3 show different shapes including unimodal, J, reverse-J, almost symmetric and positive-skewed geometry. The plots of the hrfs exhibit decreasing, increasing, inverted bathtub and bathtub shapes followed by an inverted bathtub.

Figure 4 presents 3D graphs illustrating the skewness and kurtosis of the RB-TL-TII-

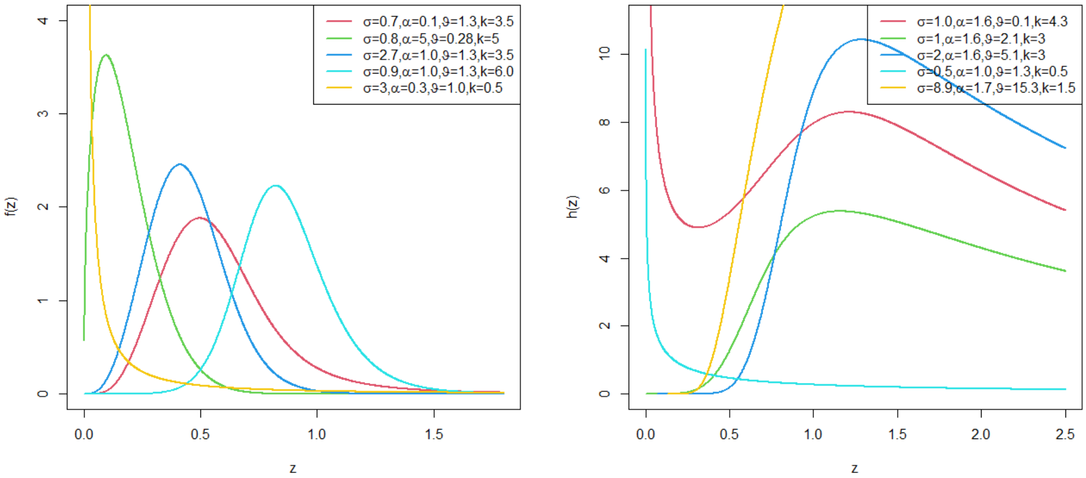

Figure 3: RB-TII-EHL-TL-LLoG pdf and hrf plots

EHL-LLoG distribution. The graphs show that if we fix ϑ and λ, both skewness and and kurtosis are low for low values of α and σ. This is an indication of symmetrical and light tailed form. Conversely, as α and σ, increase, both skewness and kurtosis increase, suggesting that the distribution approaches a more asymmetrical and heavy-tailed form.

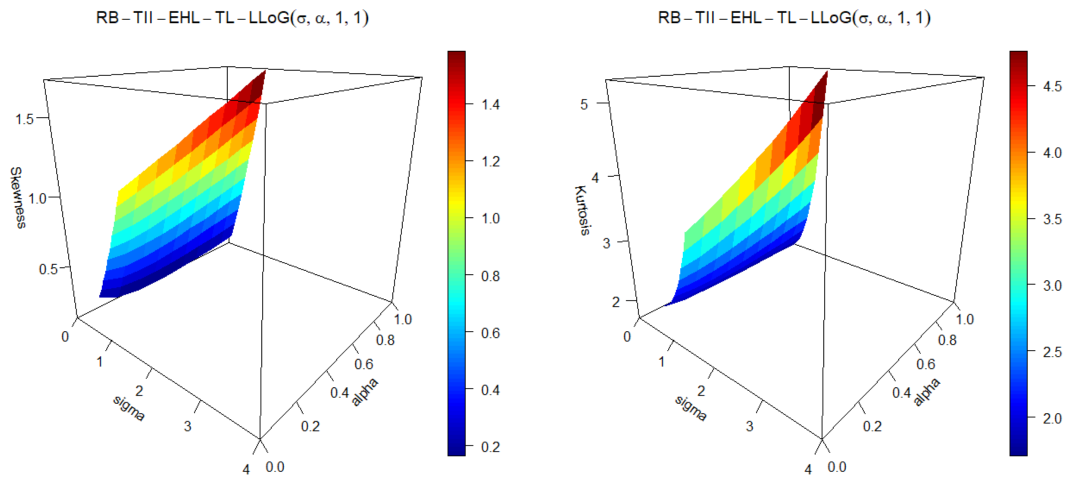

Figure 4: RB-TII-EHL-TL-LLoG: 3D Graphs of Skewness and Kurtosis

4 Additional Statistical Properties

We provide additional statistical properties of the new family of distributions including order statistics, uncertainty measure, moments and stochastic orders.

4.1 Order Statistics

Order statistics has wide applications including modeling auctions, analyzing insurance policies, optimizing production processes and estimating distribution parameters, among others.

Let $Z_1, ..., Z_n$ be independent and identically distributed RB-TII-EHL-TL-G random variables, the pdf of the i^{th} order statistics is

$$f_{i:n}(z) = \frac{\Gamma(n+1)}{\Gamma(i)\Gamma(n-i+1)} \sum_{q=0}^{\infty} \sum_{r=0}^{n-i} (-1)^r \binom{n-i}{r} a_{q+1} g_{q+1}(z; \underline{\zeta}), \tag{9}$$

where $g_{q+1}(z;\underline{\zeta}) = (q+1)g(z;\underline{\zeta})G^q(z;\underline{\zeta})$ is the Expo-G distribution with parameter $(q+1)$ and

$$\begin{aligned} a_{q+1} &= \sum_{j,m,s,k,l,t=0}^{\infty} b_{s,m} (-1)^{j+k+t+q} \left(\sum_{p=0}^{\infty} \frac{(-1)^p}{(p+\sigma)p!} \right)^j \frac{4\alpha\vartheta}{[\Gamma(\sigma)]^{j+1}} \binom{r+i-1}{j} \\ &\times \binom{j(p+\sigma)+\sigma-1}{m} \binom{\alpha[m+s+j(p+\sigma)+\sigma]-1}{k} \binom{-\alpha[m+s+j(p+\sigma)+\sigma]-1}{l} \\ &\times \binom{\vartheta(k+l+1)-1}{t} \binom{2t+1}{q} \frac{1}{(q+1)}. \end{aligned}$$

Consequently, the Expo-G distribution may be used to directly determine the distribution of the i^{th} OS of theRB-TII-EHL-TL-G family of distributions. *For derivations, please refer to the Web Appendix.*

4.2 Uncertainty Measure

A statistical distribution's level of uncertainty can be measured by the Rényi entropy (Rényi, 1961). If $Z \sim$ RB-TII-EHL-TL-G family of distributions, the Rényi entropy of order v is

$$I_R(v) = (1-v)^{-1} \log \left(\sum_{r=0}^{\infty} \psi_{r+1} e^{\{(1-v)I_{REG}\}} \right), \tag{10}$$

for $v \geq 0$ and $v \neq 1$, where

$$\begin{aligned} \psi_{r+1} &= \left(\frac{4\alpha\vartheta}{\Gamma(\sigma)} \right)^v \sum_{m,s,i,j,k=0}^{\infty} b_{s,m} (-1)^{i+k+r} \binom{v(\sigma-1)}{m} \binom{\alpha(m+s+v\sigma)-v}{i} \\ &\times \binom{-\alpha(m+s+v\sigma)-v}{j} \binom{\vartheta(i+j)+v(\vartheta-1)}{k} \binom{2k+v}{r} \frac{1}{\left[\frac{m}{v}+1\right]^v}, \end{aligned}$$

and

$$I_{REG} = (1-v)^{-1} \log \left[\int_0^{\infty} \left(\left[\frac{m}{v} + 1 \right] g(z; \underline{\zeta}) G^{\frac{m}{v}}(z; \underline{\zeta}) \right)^{v} dz \right] \tag{11}$$

is the Rényi entropy of the Expo-G distribution with parameter $\left[\frac{m}{v}+1\right]$. Consequently, the Rényi of the RB-TII-EHL-TL-G family of distributions can be found directly from the R Rényi of the Expo-G distribution. *For derivations, please refer to the Web Appendix.*

4.3 Moments

This subsection presents moments, moment generating functions (mgfs) and conditional moments of the RB-TII-EHL-TL-G family of distributions.

4.3.1 Moments and Moment Generating Functions

Let $f(z) = f_{RB-TII-EHL-TL-G}(z; \sigma, \alpha, \vartheta, \underline{\zeta})$. If $Z \sim$ RB-TII-EHL-TL-G$(\sigma, \alpha, \vartheta, \underline{\zeta})$ distribution and $Y \sim$ Expo-G$(p+1)$, the k^{th} moment $\mu_k^{'}$ is

$$\mu_k^{'} = E(Z^k) = \int_0^{\infty} z^k f(z) dz = \sum_{p=0}^{\infty} \eta_{p+1} E(Y^k),$$

where $E(Y^k)$ is the k^{th} moment of the Expo-G distribution with parameter $(p+1)$ and η_{p+1} is as given in equation (8). The mgf of RB-TII-EHL-TL-G family of distributions is obtained as follows:

$$M_Z(t) = \sum_{p=0}^{\infty} \eta_{p+1} M_Y(t),$$

where $M_Y(t)$ is the mgf of the Expo-G distribution and η_{p+1} is given by equation (8).

4.3.2 Conditional Moments

The k^{th} conditional moment for RB-TII-EHL-TL-G family of distributions is obtained as follows:

$$\begin{aligned} E(Z^k | Z > t) &= \frac{1}{\bar{F}(t)} \int_t^{\infty} z^k f(z) dz \\ &= \sum_{p=0}^{\infty} \eta_{p+1} E(Y^k I_{\{Y^k > t\}}), \end{aligned}$$

where $E(Y^k I_{\{Y^k > t\}}) = \int_t^{\infty} y^k g_{p+1}(y; \underline{\zeta}) dy$ and η_{p+1} is given by equation (8).

4.4 Stochastic Orders

Stochastic ordering has wide applications in statistics and statistical decision theory. It is useful in deducing probability inequalities, comparing stochastic models, establishing bounds and inequalities in reliability. It is very useful in hypothesis testing, simultaneous comparisons and multiple decision problems. Stochastic ordering is also useful in economics in the area of decisions under risk, particularly in the context of multi-attribute utility theory.

In this subsection, we present stochastic orders for the RB-TII-EHL-TL-G family of distributions. Let Z_1 and Z_2 be two random variables with cdfs $F_{Z_1}(u)$ and $F_{Z_2}(u)$. We say that Z_1 is stochastically smaller than Z_2 if $\overline{F}_1(u) \le \overline{F}_2(u)$ or equivalently $F_{Z_1}(u) \ge F_{Z_2}(u)$ $\forall u$, where $\overline{F}_1(u)$ and $\overline{F}_2(u)$ are survival functions of Z_1 and Z_2, respectively. The hazard rate (hr) order and the likelihood ratio (lr) order are $Z_1 <_{hr} Z_2$ if $h_{Z_1}(u) \ge h_{Z_2}(u)$ and $Z_1 <_{lr} Z_2$ if $\frac{f_{Z_1}(u)}{f_{Z_2}(u)}$ is decreasing in u. It is also well known that $Z_1 <_{l_r} Z_2 \Rightarrow Z_1 <_{h_r} Z_2 \Rightarrow Z_1 <_{st} Z_2$, (Shaked and Shanthikumar, 2007).

Theorem 1. *Let $Z_1 \sim$ RB-TII-EHL-TL-G $(\sigma_1, \alpha, \vartheta; \underline{\zeta})$ and $Z_2 \sim$ RB-TII-EHL-TL-G $(\sigma_2, \alpha, \vartheta; \underline{\zeta})$, if $\sigma_1 \le \sigma_2$, then $\frac{f(z;\sigma_1,\alpha,\vartheta,\underline{\zeta})}{f(z;\sigma_2,\alpha,\vartheta,\underline{\zeta})}$ is decreasing in z.*

Proof of Theorem 1: Consider two independent random variables Z_1 and Z_2 with pdfs

$$
\begin{aligned}
f(z;\sigma_1,\alpha,\vartheta,\underline{\zeta}) &= \frac{4\alpha\vartheta}{\Gamma(\sigma_1)}\left(-\log\left[1-W_G(z;\alpha,\vartheta,\underline{\zeta})\right]\right)^{\sigma_1-1} \\
&\times \frac{g(z;\underline{\zeta})[1-\bar{G}^2(z;\underline{\zeta})]^{\vartheta-1}\bar{G}(z;\underline{\zeta})\left(1-[1-\bar{G}^2(z;\underline{\zeta})]^{\vartheta}\right)^{\alpha-1}}{(1+[1-\bar{G}^2(z;\underline{\zeta})]^{\vartheta})^{\alpha+1}},
\end{aligned}
$$

and

$$
\begin{aligned}
f(z;\sigma_2,\alpha,\vartheta,\underline{\zeta}) &= \frac{4\alpha\vartheta}{\Gamma(\sigma_2)}\left(-\log\left[1-W_G(z;\alpha,\vartheta,\underline{\zeta})\right]\right)^{\sigma_2-1} \\
&\times \frac{g(z;\underline{\zeta})[1-\bar{G}^2(z;\underline{\zeta})]^{\vartheta-1}\bar{G}(z;\underline{\zeta})\left(1-[1-\bar{G}^2(z;\underline{\zeta})]^{\vartheta}\right)^{\alpha-1}}{(1+[1-\bar{G}^2(z;\underline{\zeta})]^{\vartheta})^{\alpha+1}}.
\end{aligned}
$$

Then,

$$
\begin{aligned}
\frac{f(z;\sigma_1,\alpha,\vartheta,\underline{\zeta})}{f(z;\sigma_2,\alpha,\vartheta,\underline{\zeta})} &= \frac{\Gamma(\sigma_2)}{\Gamma(\sigma_1)}\frac{\left(-\log\left[1-W_G(z;\alpha,\vartheta,\underline{\zeta})\right]\right)^{\sigma_1-1}}{\left(-\log\left[1-W_G(z;\alpha,\vartheta,\underline{\zeta})\right]\right)^{\sigma_2-1}} \\
&= \frac{\Gamma(\sigma_2)}{\Gamma(\sigma_1)}\left(-\log\left[1-W_G(z;\alpha,\vartheta,\underline{\zeta})\right]\right)^{\sigma_1-\sigma_2}. \qquad (12)
\end{aligned}
$$

The derivative of Equation (12) with respect to z is

$$\begin{aligned}\frac{d}{dz}\left(\frac{f(z;\sigma_1,\alpha,\vartheta,\underline{\zeta})}{f(z;\sigma_2,\alpha,\vartheta,\underline{\zeta})}\right) &= 4abg(z;\underline{\zeta})(\sigma_2-\sigma_1)\frac{\Gamma(\sigma_2)}{\Gamma(\sigma_1)} \\ &\times \left(-\log\left[1-W_G(z;\alpha,\vartheta,\underline{\zeta})\right]\right)^{\sigma_1-\sigma_2-1} \\ &\times \frac{[1-\bar{G}^2(z;\underline{\zeta})]^{b-1}\bar{G}(z;\underline{\zeta})}{\left[1-W_G(z;\alpha,\vartheta,\underline{\zeta})\right]} \\ &\times \frac{\left(1-[1-\bar{G}^2(z;\underline{\zeta})]^{\vartheta}\right)^{\alpha-1}}{\left(1+[1-\bar{G}^2(z;\underline{\zeta})]^{\vartheta}\right)^{\alpha+1}}.\end{aligned}$$

Now, $\frac{d}{dz}\left(\frac{f(z;\sigma_1,\alpha,\vartheta,\underline{\zeta})}{f(z;\sigma_2,\alpha,\vartheta,\underline{\zeta})}\right) < 0$ if $\sigma_2 < \sigma_1$. Therefore, $Z_1 <_{l_r} Z_2$ and consequently, $Z_1 <_{h_r} Z_2$ and $Z_1 <_{st} Z_2$. We can conclude that the random variables Z_1 and Z_2 are stochastically ordered.

5 Parameter Estimation

We examine various approaches used to estimate the parameters of RB-TII-EHL-TL-G family of distributions. These include the Anderson-Darling (AD), least squares (LS), Cramér-von-Mises (CVM) and maximum likelihood (ML) method.

5.1 ML Estimation

Let Z $\sim$RB-TII-EHL-TL-G$(\sigma,\alpha,\vartheta,\underline{\zeta})$ and $\mathbf{\Lambda} = (\sigma,\alpha,\vartheta,\underline{\zeta})^T$ be the vector of model parameters, the log-likelihood function $\ell = \ell(\mathbf{\Lambda})$ is

$$\begin{aligned}\ell(\mathbf{\Lambda}) &= n\ln(4\alpha\vartheta) + (\sigma-1)\sum_{i=1}^{n}\ln\left(-\log\left[1-W_G(z;\alpha,\vartheta,\underline{\zeta})\right]\right) \\ &- n\ln[\Gamma(\sigma)] + \sum_{i=1}^{n}\ln[g(z_i;\underline{\zeta})] + (\vartheta-1)\sum_{i=1}^{n}\ln[1-\bar{G}^2(z_i;\underline{\zeta})] \\ &+ \sum_{i=1}^{n}\ln[\bar{G}(z_i;\underline{\zeta})] + (\alpha-1)\sum_{i=1}^{n}\ln\left(1-[1-\bar{G}^2(z_i;\underline{\zeta})]^{\vartheta}\right) \\ &- (\alpha+1)\sum_{i=1}^{n}\ln(1+[1-\bar{G}^2(z_i;\underline{\zeta})]^{\alpha}).\end{aligned} \tag{13}$$

The ML parameter estimates are found by solving the nonlinear system of equations $\left[\frac{\partial\ell(\mathbf{\Lambda})}{\partial\sigma}, \frac{\partial\ell(\mathbf{\Lambda})}{\partial\alpha}, \frac{\partial\ell(\mathbf{\Lambda})}{\partial\vartheta}, \frac{\partial\ell(\mathbf{\Lambda})}{\partial\underline{\zeta}_k}\right]^T = \mathbf{0}$, using numerical methods like Newton-Raphson procedure. *See the Web Appendix for the elements of the score vector.*

5.2 LS Estimation

The LS (Swain et al., 1988) method can be categorized into two methods: ordinary least squares (OLS) and weighted least squares (WLS). The OLS parameter estimates are obtained by minimizing

$$OLS(\mathbf{\Lambda}) = \sum_{i=1}^{n}\left(\left[1-\frac{\gamma\left(\sigma,-\log\left[1-W_G(z_{(i)};\alpha,\vartheta,\underline{\zeta})\right]\right)}{\Gamma(\sigma)}\right]-p_i\right)^2,$$

with respect to σ, a, ϑ, and $\underline{\zeta}$, where $p_i=\frac{i}{n+1}$. To find the OLS parameter estimates, we solve the nonlinear system of equations

$$\left[\frac{\partial OLS(\mathbf{\Lambda})}{\partial\sigma},\frac{\partial OLS(\mathbf{\Lambda})}{\partial\alpha},\frac{\partial OLS(\mathbf{\Lambda})}{\partial\vartheta},\frac{\partial OLS(\mathbf{\Lambda})}{\partial\underline{\zeta}_k}\right]^T=\mathbf{0},$$

using numerical methods like Newton-Raphson procedure. The WLS parameter estimates are obtained by minimizing

$$WLS(\mathbf{\Lambda}) = \sum_{i=1}^{n}\omega_i\left(\left[1-\frac{\gamma\left(\sigma,-\log\left[1-W_G(z_{(i)};\alpha,\vartheta,\underline{\zeta})\right]\right)}{\Gamma(\sigma)}\right]-p_i\right)^2,$$

with respect to $\sigma, a, \vartheta, \underline{\zeta}$, where $\omega_i=\frac{(n+1)^2(n+2)}{i(n-i+1)}$. To find the WLS parameter estimates, we solve the nonlinear system of equations

$$\left[\frac{\partial WLS(\mathbf{\Lambda})}{\partial\sigma},\frac{\partial WLS(\mathbf{\Lambda})}{\partial\alpha},\frac{\partial WLS(\mathbf{\Lambda})}{\partial\vartheta},\frac{\partial WLS(\mathbf{\Lambda})}{\partial\underline{\zeta}_k}\right]^T=\mathbf{0},$$

using numerical methods like Newton-Raphson procedure.

5.3 CVM Estimation

The CVM estimation technique was proposed by Macdonald (1971). The CVM parameter estimates are obtained by minimizing

$$CVM(\mathbf{\Lambda}) = \frac{1}{12n}+\sum_{i=1}^{n}\left(\left[1-\frac{\gamma\left(\sigma,-\log\left[1-W_G(z_{(i)};\alpha,\vartheta,\underline{\zeta})\right]\right)}{\Gamma(\sigma)}\right]-q_i\right)^2,$$

with respect to σ, a, ϑ, and $\underline{\zeta}$, where $q_i=\frac{2i-1}{2n}$. To find the CVM parameter estimates, we solve the nonlinear system of equations

$$\left[\frac{\partial CVM(\mathbf{\Lambda})}{\partial\sigma},\frac{\partial CVM(\mathbf{\Lambda})}{\partial\alpha},\frac{\partial CVM(\mathbf{\Lambda})}{\partial\vartheta},\frac{\partial CVM(\mathbf{\Lambda})}{\partial\underline{\zeta}_k}\right]^T=\mathbf{0},$$

using numerical methods like Newton-Raphson procedure.

5.4 AD Estimation

The AD method of estimation was developed by Anderson and Darling (1952). The AD parameter estimates are obtained by minimizing

$$\begin{aligned} AD(\mathbf{\Lambda}) &= -n - n^{-1}\sum_{i=1}^{n}\left[r_i\log\left(1-\frac{\gamma\left(\sigma,-\log\left[1-W_G(z_{(i)};\alpha,\vartheta,\underline{\zeta})\right]\right)}{\Gamma(\sigma)}\right)\right] \\ &- n^{-1}\sum_{i=1}^{n}\left[r_i\left(\frac{\gamma\left(\sigma,-\log\left[1-W_G(z_{(i)};\alpha,\vartheta,\underline{\zeta})\right]\right)}{\Gamma(\sigma)}\right)\right], \end{aligned}$$

with respect to σ, a, ϑ, and $\underline{\zeta}$, where $r_i = (2i-1)$. The AD parameter estimates are found by solving the nonlinear system of equations

$$\left[\frac{\partial AD(\mathbf{\Lambda})}{\partial\sigma}, \frac{\partial AD(\mathbf{\Lambda})}{\partial\alpha}, \frac{\partial AD(\mathbf{\Lambda})}{\partial\vartheta}, \frac{\partial AD(\mathbf{\Lambda})}{\partial\underline{\zeta}_k}\right]^T = \mathbf{0},$$

using numerical methods like Newton-Raphson procedure.

6 Simulation Study

We present simulation results for the various estimation techniques. Several simulations were run for different sample sizes in order to assess the performance of the estimators of RB-TII-EHL-TL-W distribution, a special case of the RB-TII-EHL-TL-G family of distributions. The root mean square error (RMSE) and average bias (ABias) were used as metrics to assess the estimators' performance. The expressions for RMSE and ABias for the estimated parameter, say, $\hat{\Omega}$ are

$\text{RMSE}(\hat{\Omega}) = \sqrt{\frac{\sum_{i=1}^{N}(\hat{\Omega}_i-\Omega)^2}{N}}$, and $\text{ABias}(\hat{\Omega}) = \frac{\sum_{i=1}^{N}\hat{\Omega}_i}{N} - \Omega$.

Tables 2 and 3 show Abias and RMSE simulation results for different estimation methods for some selected parameter values. The superscript in both tables indicates the rank of each estimator. For instance, the Abias of $\hat{\sigma}$ computed using the ML estimation technique for $n = 30$ ranks 5^{th} among all the other estimators in Table 2. The cumulative sum of the ranks is indicated by the row $\sum$ranks. Table 4 presents the combined rankings for RMSE and Abias. The superscript denotes the combined rank for each estimation method. The partial sum of the ranks is shown by the row with the label $\sum$ranks.

From Tables 2 and 3, we can conclude that, generally, the RMSE decreases as sample size (n) increases. However, the Abias occasionally decreases with increasing n. Based on the results in Table 4, the ML estimation method ranks the highest, followed by OLS method. According to the rankings, the AD method is the lowest.

Figures 5 and 6 display the RMSE plots which illustrate how the RMSEs of the RB-TII-EHL-TL-W parameters change with increasing n for different estimation techniques.

For all the five estimation techniques examined, the graphs show that as n increases, the RMSE consistently decrease, indicating improved accuracy in parameter estimation.

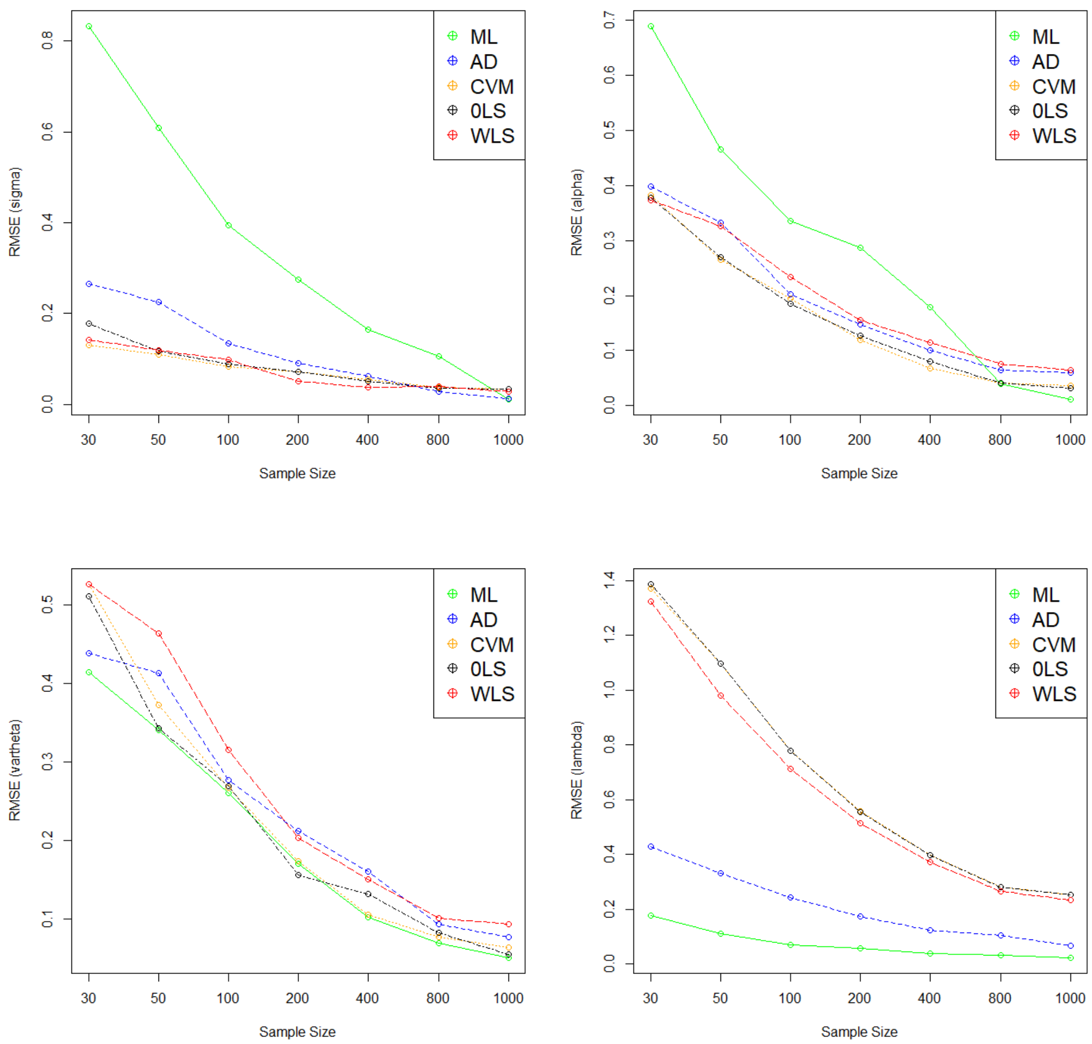

Figure 5: RB-TII-EHL-TL-W RMSE Graphs for $\sigma, \alpha, \vartheta, \lambda$ from Table 2

Table 2: RB-TII-EHL-TL-W Simulation Results for $\sigma = 0.3, \alpha = 0.7, \vartheta = 0.7, \lambda = 0.8$

		RMSE					Abias				
Parameter	n	ML	AD	CVM	OLS	WLS	MLE	AD	CVM	OLS	WLS
σ	30	0.8339 $^{(5)}$	0.2647 $^{(4)}$	0.1308 $^{(1)}$	0.1787 $^{(3)}$	0.1413 $^{(2)}$	0.3093 $^{(5)}$	0.1263 $^{(4)}$	0.1031 $^{(2)}$	0.1100 $^{(3)}$	0.0487 $^{(1)}$
α	30	0.6901 $^{(5)}$	0.3986 $^{(4)}$	0.3831 $^{(3)}$	0.3785 $^{(2)}$	0.3730 $^{(1)}$	0.0713 $^{(1)}$	0.1585 $^{(5)}$	0.0752 $^{(3)}$	0.0766 $^{(4)}$	0.0713 $^{(2)}$
ϑ	30	0.4140 $^{(1)}$	0.4389 $^{(2)}$	0.5269 $^{(5)}$	0.5107 $^{(3)}$	0.5266 $^{(4)}$	0.3618 $^{(5)}$	-0.0431 $^{(4)}$	-0.0128 $^{(1)}$	-0.0158 $^{(2)}$	-0.0260 $^{(3)}$
λ	30	0.1778 $^{(1)}$	0.4280 $^{(2)}$	1.3700 $^{(4)}$	1.3887 $^{(5)}$	1.3246 $^{(3)}$	-0.0283 $^{(1)}$	-0.2389 $^{(2)}$	-0.7784 $^{(5)}$	-0.7779 $^{(4)}$	-0.7107 $^{(3)}$
$\sum$ranks		12	12	13	13	10	12	15	11	13	9
σ	50	0.6089 $^{(5)}$	0.2257 $^{(4)}$	0.1091 $^{(1)}$	0.1178 $^{(2)}$	0.1195 $^{(3)}$	0.2028 $^{(5)}$	0.1333 $^{(4)}$	0.0548 $^{(2)}$	0.0605 $^{(3)}$	0.0425 $^{(1)}$
α	50	0.4659 $^{(5)}$	0.3318 $^{(4)}$	0.2647 $^{(1)}$	0.2702 $^{(2)}$	0.3268 $^{(3)}$	0.0524 $^{(1)}$	0.1298 $^{(5)}$	0.0588 $^{(3)}$	0.0572 $^{(2)}$	0.0689 $^{(4)}$
ϑ	50	0.3405 $^{(1)}$	0.4129 $^{(4)}$	0.3722 $^{(3)}$	0.3427 $^{(2)}$	0.4643 $^{(5)}$	0.1717 $^{(5)}$	-0.0884 $^{(4)}$	-0.0276 $^{(3)}$	-0.0072 $^{(1)}$	-0.0241 $^{(2)}$
λ	50	0.1110 $^{(1)}$	0.3316 $^{(2)}$	1.0967 $^{(5)}$	1.0966 $^{(4)}$	0.9802 $^{(3)}$	-0.0278 $^{(1)}$	-0.2331 $^{(2)}$	-0.7763 $^{(5)}$	-0.7741 $^{(4)}$	-0.6709 $^{(3)}$
$\sum$ranks		12	14	10	10	14	12	15	13	10	10
σ	100	0.3949 $^{(5)}$	0.1343 $^{(4)}$	0.0827 $^{(1)}$	0.0883 $^{(2)}$	0.0979 $^{(3)}$	0.1202 $^{(4)}$	0.1231 $^{(5)}$	0.0583 $^{(3)}$	0.0578 $^{(2)}$	0.0488 $^{(1)}$
α	100	0.3352 $^{(5)}$	0.2025 $^{(3)}$	0.1949 $^{(2)}$	0.1853 $^{(1)}$	0.2331 $^{(4)}$	0.0236 $^{(1)}$	0.1544 $^{(5)}$	0.0575 $^{(3)}$	0.0573 $^{(2)}$	0.0913 $^{(4)}$
ϑ	100	0.2600 $^{(1)}$	0.2769 $^{(4)}$	0.2671 $^{(2)}$	0.2695 $^{(3)}$	0.3151 $^{(5)}$	0.0909 $^{(4)}$	-0.0962 $^{(5)}$	-0.0038 $^{(2)}$	-0.0026 $^{(1)}$	0.0183 $^{(3)}$
λ	100	0.0707 $^{(1)}$	0.2417 $^{(2)}$	0.7776 $^{(4)}$	0.7790 $^{(5)}$	0.7126 $^{(3)}$	-0.0273 $^{(1)}$	-0.2414 $^{(2)}$	-0.7763 $^{(4)}$	-0.7774 $^{(5)}$	-0.7002 $^{(3)}$
$\sum$ranks		12	13	9	11	15	10	17	12	10	11
σ	200	0.2751 $^{(5)}$	0.0904 $^{(4)}$	0.0716 $^{(2)}$	0.0720 $^{(3)}$	0.0508 $^{(1)}$	0.0461 $^{(1)}$	0.1139 $^{(5)}$	0.0768 $^{(3)}$	0.0796 $^{(4)}$	0.0463 $^{(2)}$
α	200	0.2869 $^{(5)}$	0.1482 $^{(3)}$	0.1189 $^{(1)}$	0.1279 $^{(2)}$	0.1560 $^{(4)}$	0.0118 $^{(1)}$	0.1266 $^{(5)}$	0.0272 $^{(2)}$	0.0388 $^{(3)}$	0.0992 $^{(4)}$
ϑ	200	0.1704 $^{(1)}$	0.2124 $^{(5)}$	0.1738 $^{(2)}$	0.1557 $^{(3)}$	0.2032 $^{(4)}$	0.0664 $^{(4)}$	-0.1066 $^{(5)}$	-0.0036 $^{(1)}$	0.0041 $^{(3)}$	0.0304 $^{(2)}$
λ	200	0.0572 $^{(1)}$	0.1726 $^{(2)}$	0.5568 $^{(5)}$	0.5563 $^{(4)}$	0.5153 $^{(3)}$	-0.0207 $^{(1)}$	-0.2439 $^{(2)}$	-0.7718 $^{(4)}$	-0.7765 $^{(5)}$	-0.7198 $^{(3)}$
$\sum$ranks		12	14	10	12	12	7	17	10	15	11
σ	400	0.1650 $^{(5)}$	0.0613 $^{(4)}$	0.0538 $^{(3)}$	0.0509 $^{(2)}$	0.0364 $^{(1)}$	0.0299 $^{(1)}$	0.1097 $^{(5)}$	0.0951 $^{(4)}$	0.0755 $^{(3)}$	0.0399 $^{(2)}$
α	400	0.1795 $^{(5)}$	0.1001 $^{(3)}$	0.0685 $^{(1)}$	0.0802 $^{(2)}$	0.1146 $^{(4)}$	0.0026 $^{(1)}$	0.1244 $^{(5)}$	-0.0036 $^{(2)}$	0.0222 $^{(3)}$	0.1116 $^{(4)}$
ϑ	400	0.1026 $^{(1)}$	0.1606 $^{(5)}$	0.1060 $^{(2)}$	0.1314 $^{(3)}$	0.1505 $^{(4)}$	0.0084 $^{(1)}$	-0.1477 $^{(5)}$	0.0213 $^{(3)}$	0.0088 $^{(2)}$	0.0405 $^{(4)}$
λ	400	0.0394 $^{(1)}$	0.1233 $^{(2)}$	0.3964 $^{(5)}$	0.3960 $^{(4)}$	0.3723 $^{(3)}$	-0.0173 $^{(1)}$	-0.2465 $^{(2)}$	-0.7927 $^{(5)}$	-0.7918 $^{(4)}$	-0.7370 $^{(3)}$
$\sum$ranks		12	14	11	11	12	4	17	14	12	13
σ	800	0.1049 $^{(5)}$	0.0277 $^{(1)}$	0.0372 $^{(3)}$	0.0360 $^{(2)}$	0.0387 $^{(4)}$	0.0123 $^{(1)}$	0.0599 $^{(3)}$	0.0910 $^{(5)}$	0.0803 $^{(4)}$	0.0523 $^{(2)}$
α	800	0.0401 $^{(1)}$	0.0653 $^{(4)}$	0.0411 $^{(2)}$	0.0417 $^{(3)}$	0.0755 $^{(5)}$	0.0026 $^{(1)}$	0.0447 $^{(4)}$	-0.0092 $^{(2)}$	0.0100 $^{(3)}$	0.0941 $^{(5)}$
ϑ	800	0.0691 $^{(1)}$	0.0935 $^{(4)}$	0.0773 $^{(2)}$	0.0828 $^{(3)}$	0.1007 $^{(5)}$	0.0089 $^{(1)}$	-0.1123 $^{(5)}$	0.0090 $^{(1)}$	0.0138 $^{(3)}$	0.0386 $^{(4)}$
λ	800	0.0323 $^{(1)}$	0.1046 $^{(2)}$	0.2811 $^{(5)}$	0.2806 $^{(4)}$	0.2649 $^{(3)}$	-0.0135 $^{(1)}$	-0.2329 $^{(2)}$	-0.7950 $^{(5)}$	-0.7937 $^{(4)}$	-0.7439 $^{(3)}$
$\sum$ranks		8	11	12	12	17	4	14	13	16	13
σ	1000	0.0103 $^{(1)}$	0.0135 $^{(2)}$	0.0327 $^{(4)}$	0.0333 $^{(5)}$	0.0277 $^{(3)}$	0.0070 $^{(1)}$	0.0413 $^{(2)}$	0.0885 $^{(4)}$	0.0975 $^{(5)}$	0.0599 $^{(3)}$
α	1000	0.0110 $^{(1)}$	0.0594 $^{(4)}$	0.0371 $^{(3)}$	0.0325 $^{(2)}$	0.0653 $^{(5)}$	0.0012 $^{(1)}$	0.0332 $^{(3)}$	-0.007323468 $^{(2)}$	-0.0115 $^{(4)}$	0.0447 $^{(5)}$
ϑ	1000	0.0503 $^{(1)}$	0.0765 $^{(3)}$	0.0639 $^{(4)}$	0.0547 $^{(2)}$	0.0935 $^{(5)}$	0.0081 $^{(2)}$	-0.1010 $^{(5)}$	0.0300 $^{(4)}$	0.0213 $^{(3)}$	0.0011 $^{(1)}$
λ	1000	0.0217 $^{(1)}$	0.0654 $^{(2)}$	0.2513 $^{(3)}$	0.2516 $^{(4)}$	0.2346 $^{(5)}$	-0.0097 $^{(1)}$	-0.2235 $^{(2)}$	-0.7947 $^{(5)}$	-0.7906 $^{(4)}$	-0.7329 $^{(3)}$
$\sum$ranks		4	11	14	13	18	5	12	15	16	12

Table 3: RB-TII-EHL-TL-W Simulation Results for $\sigma = 0.2, \alpha = 0.8, \vartheta = 0.8, \lambda = 0.8$

				RMSE					Abias		
Parameter	n	ML	AD	CVM	LSE	WLSE	MLE	AD	CVM	LSE	WLSE
σ	30	0.3890 $^{(5)}$	0.2558 $^{(4)}$	0.2376 $^{(3)}$	0.1510 $^{(1)}$	0.2163 $^{(2)}$	0.1270 $^{(4)}$	0.1272 $^{(5)}$	0.1158 $^{(3)}$	0.1077 $^{(2)}$	0.1039 $^{(1)}$
α	30	0.3993 $^{(5)}$	0.3060 $^{(3)}$	0.2884 $^{(2)}$	0.2090 $^{(1)}$	0.3331 $^{(4)}$	0.0810 $^{(5)}$	0.0559 $^{(2)}$	0.0269 $^{(1)}$	0.0674 $^{(4)}$	0.0646 $^{(3)}$
ϑ	30	0.6882 $^{(5)}$	0.4565 $^{(2)}$	0.5302 $^{(4)}$	0.3461 $^{(1)}$	0.5291 $^{(3)}$	0.2544 $^{(5)}$	-0.0520 $^{(3)}$	-0.1094 $^{(4)}$	-0.0487 $^{(2)}$	-0.0381 $^{(1)}$
λ	30	0.1157 $^{(1)}$	0.4303 $^{(2)}$	1.3797 $^{(5)}$	0.9575 $^{(3)}$	1.2923 $^{(4)}$	-0.0552 $^{(1)}$	-0.2344 $^{(2)}$	-0.7479 $^{(5)}$	-0.7365 $^{(4)}$	-0.6874 $^{(3)}$
$\sum$ranks		16	11	14	6	13	15	12	13	12	8
σ	50	0.1269 $^{(1)}$	0.1767 $^{(4)}$	0.1865 $^{(5)}$	0.1311 $^{(2)}$	0.1583 $^{(3)}$	0.0550 $^{(1)}$	0.1149 $^{(3)}$	0.1198 $^{(5)}$	0.1150 $^{(4)}$	0.1003 $^{(2)}$
α	50	0.2177 $^{(2)}$	0.2440 $^{(5)}$	0.2229 $^{(3)}$	0.1570 $^{(1)}$	0.2350 $^{(4)}$	0.0729 $^{(4)}$	0.0759 $^{(5)}$	0.0463 $^{(2)}$	0.0335 $^{(1)}$	0.0712 $^{(3)}$
ϑ	50	0.4744 $^{(5)}$	0.3794 $^{(2)}$	0.3887 $^{(3)}$	0.3036 $^{(1)}$	0.4265 $^{(4)}$	0.1740 $^{(5)}$	-0.0680 $^{(3)}$	-0.0554 $^{(2)}$	-0.1094 $^{(4)}$	-0.0486 $^{(1)}$
λ	50	0.1008 $^{(1)}$	0.3342 $^{(2)}$	1.0857 $^{(5)}$	0.7602 $^{(4)}$	0.6972 $^{(3)}$	-0.0532 $^{(1)}$	-0.2347 $^{(2)}$	-0.7657 $^{(5)}$	-0.7516 $^{(4)}$	-0.6874 $^{(3)}$
$\sum$ranks		9	13	16	8	14	11	13	14	13	9
σ	100	0.0464 $^{(1)}$	0.1279 $^{(4)}$	0.1321 $^{(5)}$	0.1025 $^{(2)}$	0.1127 $^{(3)}$	0.0056 $^{(1)}$	0.1155 $^{(3)}$	0.1213 $^{(4)}$	0.1258 $^{(5)}$	0.1035 $^{(2)}$
α	100	0.1204 $^{(1)}$	0.1563 $^{(3)}$	0.1647 $^{(4)}$	0.1219 $^{(2)}$	0.1900 $^{(5)}$	0.0221 $^{(2)}$	0.0721 $^{(5)}$	0.0311 $^{(3)}$	-0.0017 $^{(1)}$	0.0383 $^{(4)}$
ϑ	100	0.2215 $^{(1)}$	0.2878 $^{(3)}$	0.2893 $^{(4)}$	0.2330 $^{(2)}$	0.3349 $^{(5)}$	0.0757 $^{(2)}$	-0.0991 $^{(4)}$	-0.0726 $^{(1)}$	-0.1198 $^{(5)}$	-0.0839 $^{(3)}$
λ	100	0.0468 $^{(1)}$	0.2394 $^{(2)}$	0.7748 $^{(5)}$	0.5491 $^{(3)}$	0.6946 $^{(4)}$	-0.0274 $^{(1)}$	-0.2382 $^{(2)}$	-0.7736 $^{(3)}$	-0.7750 $^{(4)}$	-0.6777 $^{(5)}$
$\sum$ranks		4	12	18	9	17	6	14	11	15	14
σ	200	0.0293 $^{(1)}$	0.0899 $^{(4)}$	0.0910 $^{(5)}$	0.0610 $^{(2)}$	0.0866 $^{(3)}$	0.0005 $^{(1)}$	0.1163 $^{(4)}$	0.1208 $^{(5)}$	0.1064 $^{(2)}$	0.1138 $^{(3)}$
α	200	0.0597 $^{(1)}$	0.1101 $^{(4)}$	0.0992 $^{(3)}$	0.0709 $^{(2)}$	0.1287 $^{(5)}$	0.0083 $^{(1)}$	0.1027 $^{(5)}$	0.0518 $^{(2)}$	0.0648 $^{(3)}$	0.0667 $^{(4)}$
ϑ	200	0.1408 $^{(1)}$	0.1605 $^{(3)}$	0.1849 $^{(4)}$	0.1498 $^{(2)}$	0.1949 $^{(5)}$	0.0161 $^{(2)}$	-0.0284 $^{(3)}$	-0.0380 $^{(4)}$	-0.0533 $^{(5)}$	-0.0027 $^{(1)}$
λ	200	0.0372 $^{(1)}$	0.1716 $^{(2)}$	0.5541 $^{(5)}$	0.3904 $^{(3)}$	0.5146 $^{(4)}$	-0.0189 $^{(1)}$	-0.2421 $^{(2)}$	-0.7831 $^{(5)}$	-0.7802 $^{(3)}$	-0.7183 $^{(4)}$
$\sum$ranks		4	13	17	9	17	5	14	16	13	12
σ	400	0.0084 $^{(1)}$	0.0615 $^{(4)}$	0.0626 $^{(5)}$	0.0449 $^{(2)}$	0.0562 $^{(3)}$	-0.0004 $^{(1)}$	0.1079 $^{(4)}$	0.1064 $^{(3)}$	0.1086 $^{(5)}$	0.1003 $^{(2)}$
α	400	0.0253 $^{(1)}$	0.0637 $^{(3)}$	0.0709 $^{(4)}$	0.0406 $^{(2)}$	0.0820 $^{(5)}$	0.0033 $^{(1)}$	0.0905 $^{(4)}$	0.0888 $^{(3)}$	0.0156 $^{(2)}$	0.0996 $^{(5)}$
ϑ	400	0.0666 $^{(1)}$	0.1443 $^{(5)}$	0.1414 $^{(4)}$	0.1300 $^{(2)}$	0.1345 $^{(3)}$	0.0146 $^{(3)}$	-0.1108 $^{(4)}$	-0.0068 $^{(2)}$	-0.1673 $^{(5)}$	-0.0003 $^{(1)}$
λ	400	0.0228 $^{(1)}$	0.1236 $^{(2)}$	0.3931 $^{(5)}$	0.2802 $^{(3)}$	0.3668 $^{(4)}$	-0.0123 $^{(1)}$	-0.2471 $^{(2)}$	-0.7849 $^{(4)}$	-0.7924 $^{(5)}$	-0.7273 $^{(3)}$
$\sum$ranks		4	14	18	9	15	6	14	12	17	11
σ	800	0.0035 $^{(1)}$	0.0428 $^{(3)}$	0.0446 $^{(5)}$	0.0332 $^{(2)}$	0.0432 $^{(4}$	0.0001 $^{(1)}$	0.1144 $^{(4)}$	0.1006 $^{(2)}$	0.1038 $^{(3)}$	0.1158 $^{(5)}$
α	800	0.0046 $^{(1)}$	0.0414 $^{(3)}$	0.0488 $^{(4)}$	0.0326 $^{(2)}$	0.0587 $^{(5)}$	-0.0015 $^{(1)}$	0.0840 $^{(5)}$	0.0197 $^{(2)}$	0.0415 $^{(3)}$	0.0689 $^{(4)}$
ϑ	800	0.0821 $^{(1)}$	0.0838 $^{(2)}$	0.1442 $^{(5)}$	0.0938 $^{(4)}$	0.0935 $^{(3)}$	0.0129 $^{(2)}$	-0.1088 $^{(3)}$	-0.1924 $^{(5)}$	-0.1115 $^{(4)}$	0.0016 $^{(1)}$
λ	800	0.0116 $^{(1)}$	0.0876 $^{(2)}$	0.2806 $^{(5)}$	0.1985 $^{(4)}$	0.2642 $^{(3)}$	-0.0084 $^{(1)}$	-0.2476 $^{(2)}$	-0.7934 $^{(4)}$	-0.7939 $^{(5)}$	-0.7416 $^{(3)}$
$\sum$ranks		4	10	19	12	15	5	14	13	15	13
σ	1000	0.0010 $^{(1)}$	0.0381 $^{(4)}$	0.0373 $^{(3)}$	0.0268 $^{(2)}$	0.0385 $^{(5)}$	0.0001 $^{(1)}$	0.1141 $^{(4)}$	0.0995 $^{(3)}$	0.0870 $^{(2)}$	0.1152 $^{(5)}$
α	1000	0.0045 $^{(1)}$	0.0357 $^{(3)}$	0.0460 $^{(4)}$	0.0323 $^{(2)}$	0.0520 $^{(5)}$	0.0015 $^{(1)}$	0.0848 $^{(5)}$	0.0691 $^{(4)}$	0.0661 $^{(3)}$	0.0637 $^{(2)}$
ϑ	1000	0.0517 $^{(1)}$	0.0754 $^{(2)}$	0.1128 $^{(5)}$	0.0901 $^{(4)}$	0.0849 $^{(3)}$	0.0079 $^{(2)}$	-0.1130 $^{(4)}$	-0.1034 $^{(3)}$	-0.1324 $^{(5)}$	-0.0068 $^{(1)}$
λ	1000	0.0011 $^{(1)}$	0.0786 $^{(2)}$	0.2504 $^{(5)}$	0.1777 $^{(3)}$	0.2334 $^{(4)}$	-0.0082 $^{(1)}$	-0.2485 $^{(2)}$	-0.7915 $^{(4)}$	-0.7947 $^{(5)}$	-0.7314 $^{(3)}$
$\sum$ranks		4	11	17	11	17	5	15	14	15	11

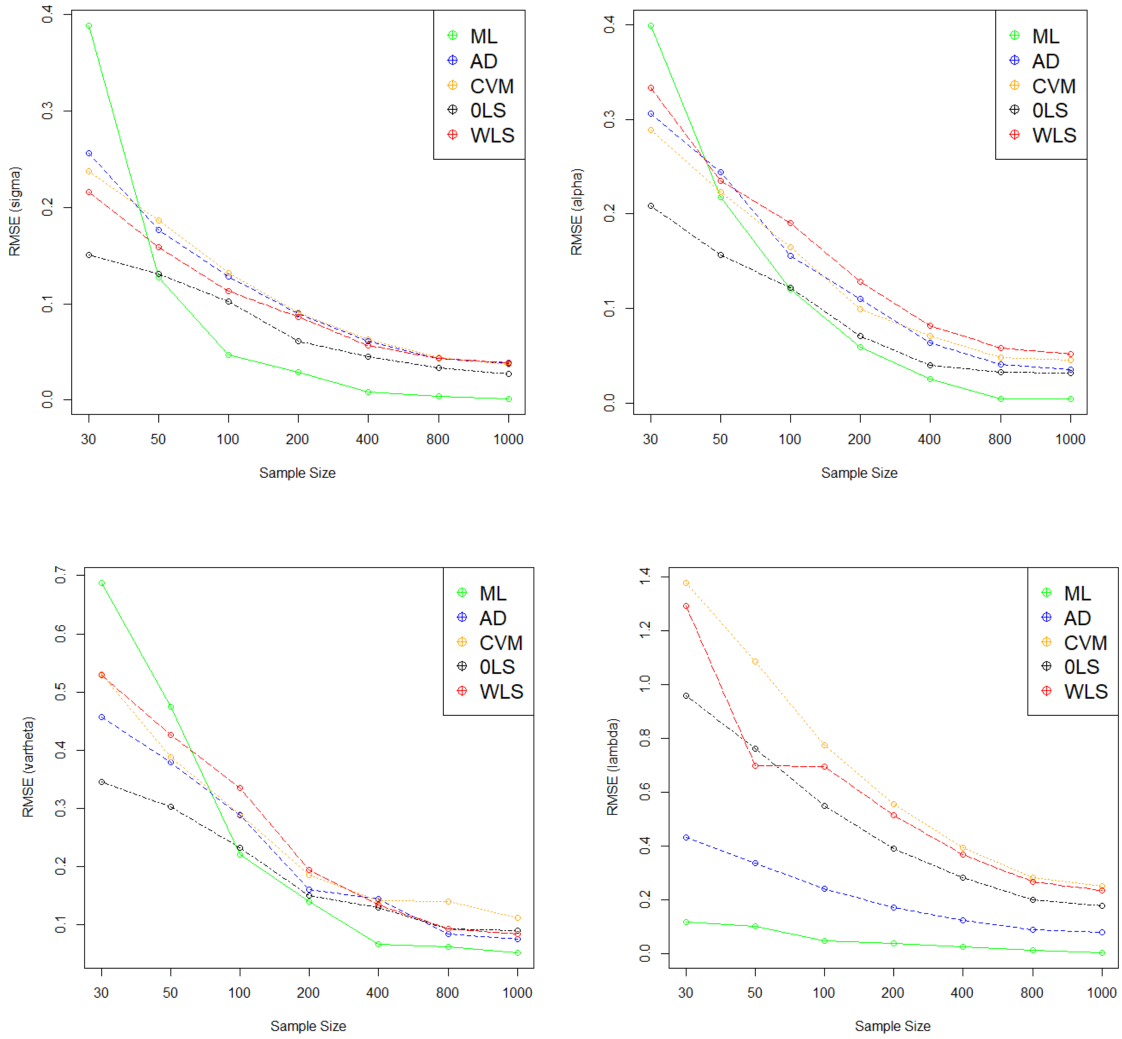

Figure 6: RB-TII-EHL-TL-W RMSE Graphs for $\sigma, \alpha, \vartheta, \lambda$ from Table 3

7 Applications

Two examples are presented to showcase the applicability, flexibility and versatility of the RB-TII-EHL-TL-W distribution. From the Monte Carlo simulation results, the ML estimation technique showed superiority performance compared to other estimation techniques, hence we employ it in estimate the model parameters. To evaluate the model, several goodness-of-fit (GoF) measures are utilized. We employ the following GoF tests: BIC, AIC, $-2\log Ł$, W^* and A^* to evaluate model performance. A high p-value and small GoF values is an indication of a good fit. We also employ the following graphs to evaluate our proposed model: empirical cumulative distribution function (ECDF)

Table 4: Partial Rank, Total Rank and Overall Rank

Parameters	n	ML	AD	CVM	LS	WLS
	30	24 $^{(2.5)}$	27 $^{(5)}$	24 $^{(2.5)}$	26 $^{(4)}$	19 $^{(1)}$
	50	24 $^{(3.5)}$	29 $^{(5)}$	23 $^{(2)}$	20 $^{(1)}$	24 $^{(3.5)}$
$\sigma = 0.3, \alpha = 0.7, \vartheta = 0.7, \lambda = 0.8$	100	22 $^{(3)}$	30 $^{(5)}$	21 $^{(1.5)}$	21 $^{(1.5)}$	26 $^{(4)}$
	200	19 $^{(1)}$	31 $^{(5)}$	20 $^{(2)}$	27 $^{(4)}$	23 $^{(3)}$
	400	16 $^{(1)}$	31 $^{(5)}$	25 $^{(3.5)}$	23 $^{(2)}$	25 $^{(3.5)}$
	800	12 $^{(1)}$	25 $^{(2.5)}$	25 $^{(2.5)}$	28 $^{(4)}$	30 $^{(5)}$
	1000	9 $^{(1)}$	23$^{(2)}$	29 $^{(3.5)}$	29 $^{(3.5)}$	30$^{(5)}$
	30	31 $^{(5)}$	23 $^{(3)}$	27 $^{(4)}$	18 $^{(1)}$	21 $^{(2)}$
	50	20 $^{(1)}$	26 $^{(4)}$	30 $^{(5)}$	21 $^{(2)}$	23 $^{(3)}$
$\sigma = 0.2, \alpha = 0.8, \vartheta = 0.8, \lambda = 0.8$	100	10 $^{(1)}$	26 $^{(3)}$	29 $^{(4)}$	24 $^{(2)}$	31 $^{(5)}$
	200	9 $^{(1)}$	27 $^{(3)}$	33 $^{(5)}$	22 $^{(2)}$	29 $^{(4)}$
	400	10 $^{(1)}$	28 $^{(4)}$	30 $^{(5)}$	26 $^{(2.5)}$	26 $^{(2.5)}$
	800	9 $^{(1)}$	24 $^{(2)}$	32 $^{(5)}$	27 $^{(3)}$	28 $^{(4)}$
	1000	9 $^{(1)}$	26 $^{(2.5)}$	31 $^{(5)}$	26 $^{(2.5)}$	28 $^{(4)}$
$\sum$ranks		24	51	45.5	35	49.5
Overall rank		1	5	3	2	4

plots, Total Time on Test (TTT) plots, Profile plots, probability-probability (PP) plots, Kaplan-Meier (K-M) survival plots, density plots and hrf plots.

We compare our proposed model with the nested and non-nested models. The following are the for parameter non-nested models: gamma Topp-Leone type II exponentiated half logistic Weibull (RBTLTIIEHLW) distribution (Oluyede and Moakofi, 2023), gamma-generalized inverse Weibull (GGIW) distribution (Oluyede et al., 2017), exponentiated half logistic odd Burr III-log-logistic (EHLOBIIILLoG) distribution (Oluyede et al., 2022b), odd Weibull-Topp-Leone-log-logistic Poisson (OWTLLLoGP) distribution (Oluyede et al., 2021), exponentiated odd Weibull-Topp-Leone-log logistic (EOWTLL-LoG) distribution (Chamunorwa et al., 2021), type II exponentiated half-logistic-Gompertz-Topp-Leone-Weibull (TIIEHLGomTLW) distribution (Oluyede and Moakofi, 2022). *See Web Appendix for the pdfs of the non-nested models.*

7.1 Italy COVID-19 Data

The COVID-19 dataset from Italy spans for 61 days and covers the period between June 13th and August 12th, 2021. It consists of the daily count of newly reported COVID-19 cases. The dataset was analyzed by Almetwally et al. (2022). The dataset is provided in the *Web Appendix.*

Results from Table 5 show that RB-TII-EHL-TL-W out performs the nested and non-nested models selected since it has the highest p-value of the K-S statistic and smallest values of all the GoF statistics. Profile plots of the ML estimates for $\sigma, \alpha, \vartheta$ and λ are presented in the *Web Appendix*. The plots demonstrate that the parameters reached their global maximum for Italy COVID-19 data. Figure 7 illustrates the fitted density plot and the PP plot Italy COVID-19 data. From the figure, it can be observed that the RB-TII-EHL-TL-W distribution's fitted density closely aligns with the sample histogram and its fitted PP plot is closer to the empirical line. This means that our proposed model is a good fit.

Table 5: Italy COVID-19 Data: Parameter Estimates and GoF Statistics

	Estimates				Statistics							
Distribution	σ	α	ϑ	λ	-2logL	AIC	CAIC	BIC	W^*	A^*	K−S	p−value
RB-TII-EHL-TL-W	7.0205×10^{-01}	$1.8798\times10^{+02}$	$9.2451\times10^{+01}$	1.1072×10^{-01}	468.9076	476.9076	477.6219	485.3511	0.0436	0.2618	0.0770	0.8627
	(3.5814×10^{-01})	(4.0054×10^{-04})	(1.6887×10^{-02})	(1.1021×10^{-02})								
RB-TII-EHL-TL-W	0.9056	0.0836	-	0.6100	554.8248	560.8249	561.2459	567.1575	0.0582	0.3258	0.3607	2.556×10^{-07}
	(0.6830)	(0.0847)	(-)	(0.0731)								
RB-TII-EHL-TL-W	0.0782	-	-	0.6008	553.8684	557.8684	558.0753	562.0902	0.0623	0.3473	0.3568	3.61×10^{-07}
	(0.0196)	(-)	(-)	(0.0703)								
RB-TII-EHL-TL-W	-	0.07171	-	0.6352	552.2675	556.2678	556.4747	560.4896	0.0569	0.3192	0.3730	8.542×10^{-08}
	(-)	(0.0198)	(-)	(0.0768)								
RB-TII-EHL-TL-W	-	-	-	0.1473	913.7705	915.7705	915.8383	917.8814	0.0948	0.5270	0.95	2.2×10^{-16}
	(-)	(-)	(-)	(0.0150)								
	δ	a	b	λ								
RBTLTIIEHLW	4.8381	0.0383	7.7882	0.7695	469.2757	477.2757	477.9899	485.7191	0.0534	0.3015	0.0885	0.7262
	(11.3379)	(0.0846)	(12.6571)	(0.5415)								
	k	β	λ	δ								
GGIW	5.3680×10^{-04}	2.9387	2.1490×10^{-01}	$7.5370\times10^{+01}$	476.6245	484.6245	485.3387	493.068	0.1655	0.9434	0.1345	0.2199
	(6.3413×10^{-04})	(1.0087×10^{-03})	(1.5921×10^{-02})	(2.9031×10^{-05})								
	a	b	α	c								
EHLOBIIILLoG	$1.8052\times10^{+01}$	$2.6030\times10^{+01}$	1.8991	9.2964×10^{-02}	488.3327	496.3327	497.0470	504.7762	0.3058	1.7760	0.1395	0.1859
	(3.7591×10^{-05})	$(2.3938\times10^{+01})$	(1.2858)	(8.0475×10^{-03})								
	α	λ	γ	θ								
OWTLLLoGP	1.9076	3.4083×10^{-01}	$1.0065\times10^{+01}$	2.6363×10^{-09}	478.8511	486.8511	487.5654	495.2946	0.0470	0.2826	0.1691	0.0610
	(2.6406×10^{-01})	(3.1629×10^{-02})	(1.5017)	(7.6817×10^{-03})								
	α	b	ϑ	c								
EOWTLLLoG	1.2889	24.5939	1.2906	0.5252	469.4652	477.4652	478.1795	485.9087	0.0591	0.3401	0.0989	0.5895
	(0.7040)	(12.4521)	(0.4312)	(0.0914)								
	α	γ	b	β								
TIIEHLGomTLW	0.0054	1.0484	1.7102	0.3122	477.7649	485.7649	486.4792	494.2084	1.3453	7.8119	0.1113	0.4371
	(0.0039)	(0.4696)	(0.0354)	(0.0678)								

Figure 8 presents the K-M Survival plot and the ECDF plot for the Italy COVID-19 data. Upon examination of both graphs, it can be observed that the RB-TII-EHL-TL-W distribution serves as a good model, since the observed and fitted values closely align with each other. Figure 9 displays the TTT scaled plot and the hrf plot for Italy COVID-19 data. The TTT scaled plot suggests an increasing hrf.

7.2 Earthquake Data

The dataset corresponds to the time intervals between consecutive earthquakes observed in the North Anatolia fault zone over the course of the past century. The data set can be accessed at the following URL: https://www.academia.edu/ 4022532/. The dataset is provided in the *Web Appendix.*

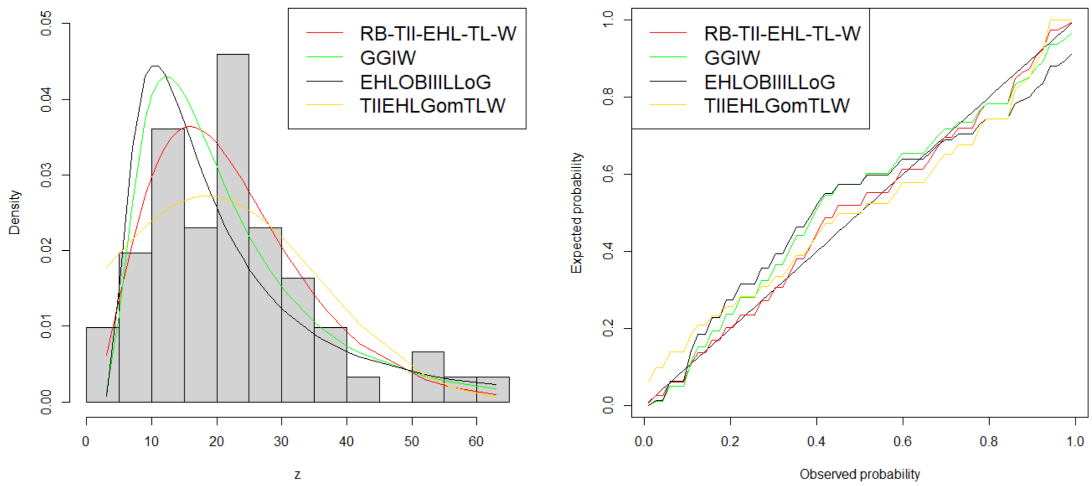

Figure 7: Fitted Densities and PP Plots for Italy COVID-19 Data

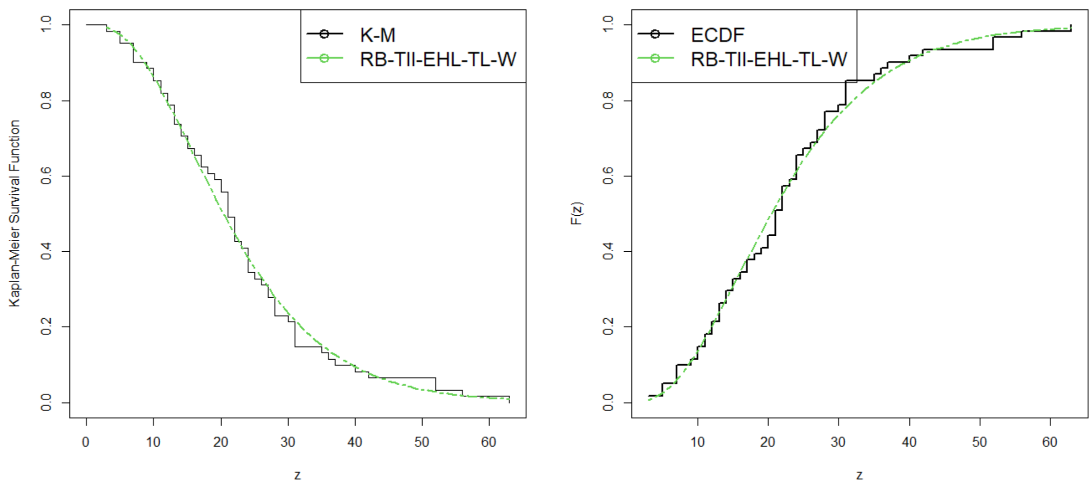

Figure 8: Fitted K-M Survival and ECDF Plots for Italy COVID-19 Data

Results of the GoF and p-values presented in Table 6 show that RB-TII-EHL-TL-W distribution demonstrates superior performance compared to the selected competing models under consideration. Profile plots of the ML estimates for $\sigma, \alpha, \vartheta$ and λ are presented at the *Web Appendix*. The plots show that the parameters are identifiable for the earthquake data.

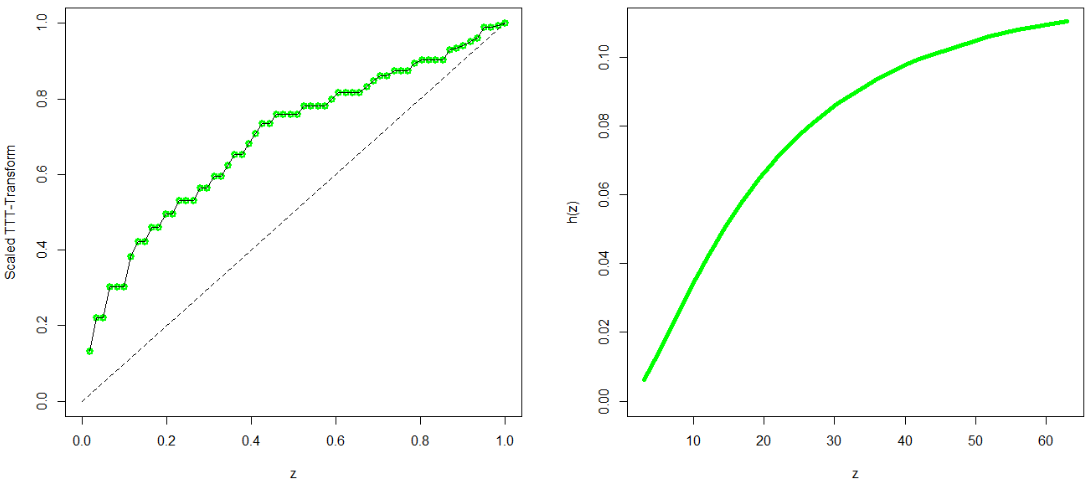

Figure 9: Fitted TTT scaled Plot and hrf Plots for Italy COVID-19 Data

Table 6: Earthquake Data: Parameter Estimates and GoF Statistics

	Estimates				Statistics							
Distribution	σ	α	ϑ	λ	-2logL	AIC	CAIC	BIC	W^*	A^*	K−S	p−value
RB-TII-EHL-TL-W	2.5945	4.9008×10^{05}	1.6549×10^{02}	2.6527×10^{-02}	393.5490	401.5490	403.6542	406.2612	0.03687	0.2219	0.0917	0.9765
	(6.4721×10^{-01})	(5.0011×10^{-07})	(3.8547×10^{-02})	(1.9746×10^{-03})								
RB-TII-EHL-TL-W	0.9950	0.0676	-	0.2809	423.3365	429.3365	430.5365	432.8707	0.0222	0.1595	0.3609	0.0026
	(0.4701)	(0.0420)	(-)	(0.0475)								
RB-TII-EHL-TL-W	0.0800	-	-	0.2710	422.9488	426.9488	427.5202	429.3049	0.0220	0.1630	0.3832	0.0011
	(0.0316)	(-)	(-)	(0.0501)								
RB-TII-EHL-TL-W	-	0.0751	-	0.2919	421.8254	425.8254	426.3968	428.1815	0.0225	0.1593	0.4159	0.0003
	(-)	(0.0375)	(-)	(0.0613)								
RB-TII-EHL-TL-W	-	-	-	0.0675	563.1342	565.1342	566.3123	566.3123	0.9123	0.5432	0.8722	2.2000×10^{-16}
	()	()	()	(0.0110)								
	σ	a	b	λ								
RBTLTIIEHLW	8.4086×10^{01}	4.7906×10^{-03}	2.2081×10^{01}	9.5945×10^{-02}	424.3662	432.3662	434.4713	437.0783	0.0259	0.4203	0.2425	0.051
	(4.0572×10^{-06})	(6.4579×10^{-04})	(2.1614×10^{-05})	(1.9437×10^{-02})								
	k	ϑ	λ	σ								
GGIW	0.0826	2.3766	0.9615	18.4605	398.7646	406.7646	408.8699	411.4768	0.0664	0.528	0.1386	0.6948
	(0.4279)	(5.5545)	(2.3891)	(9.9598)								
	a	b	α	c								
EHLOBIIILLoG	0.6669	12.9832	2.1367	1.0230	401.1430	409.1430	411.2483	413.8552	0.0909	0.6901	0.1385	0.6961
	(0.0624)	(16.6590)	(2.1110)	(0.0407)								
	α	λ	γ	θ								
OWTLLLoGP	1.9014	1.5361×10^{-01}	$1.0067\times10^{+01}$	3.4462×10^{-08}	395.4174	403.4174	405.5227	408.1297	0.0286	0.1843	0.1662	0.4712
	(4.6049×10^{-01})	(2.6460×10^{-02})	(2.7955)	(7.5868×10^{-02})								
	α	b	ϑ	c								
EOWTLLLoG	38.6703	0.0187	0.0741	1.1644	396.3042	404.3042	406.4095	409.0164	0.0364	0.3075	0.1164	0.8641
	(18.7070)	(0.0497)	(0.0393)	(0.6806)								
	α	γ	b	β								
TIIEHLGomTLW	0.0020	1.5556	1.1730	0.1110	396.1103	404.1103	406.2156	408.8226	0.89681	4.846129	0.16667	0.4678
	(0.0034)	(0.9412)	(0.0186)	(0.0382)								

Figure 10 shows that the RB-TII-EHL-TL-W's fitted density is closer to the sample histogram and its fitted PP plot is closer to the empirical line. This means that our proposed model is an adequate fit for earthquake data. The earthquake data's K-M survival plot and ECDF plot are shown in Figure 11. We conclude that our model fits the data well because the fitted and observed distributions for both graphs are fairly close to each other. Figure 12 shows concave TTT scaled plot and hrf plot for earthquake

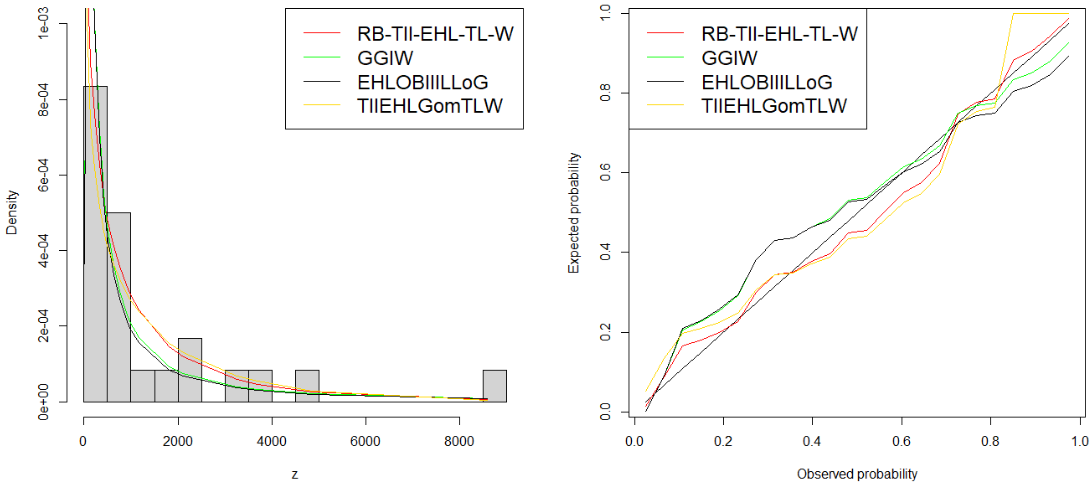

Figure 10: Fitted Densities and PP Plots for Earthquake Data

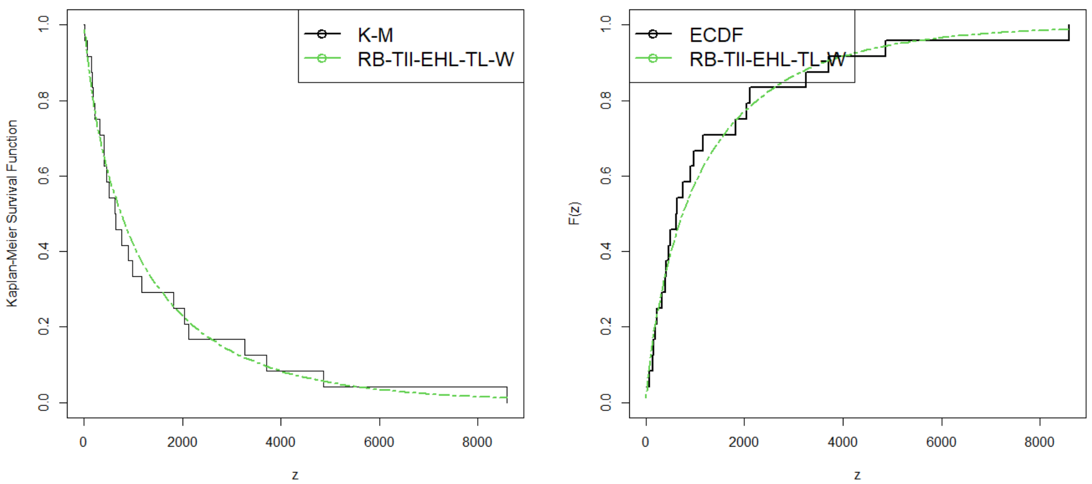

Figure 11: Fitted K-M Survival and ECDF Graphs for Earthquake Data

data. The TTT scaled plot suggests an decreasing hrf.

7.3 Likelihood Ratio (LR) Test

Table 7 presents the LR test results for Italy COVID-19 data and earthquake data. The table demonstrates the RB-TII-EHL-TL-W model outperforms the nested models at 5% significance level since all p-values for both datasets are below 0.05.

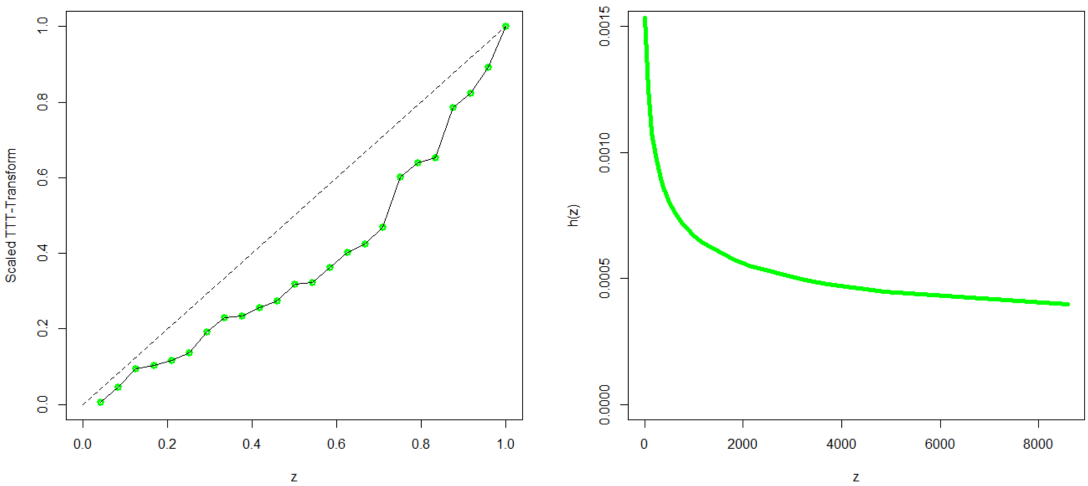

Figure 12: Earthquake Data: Fitted TTT and hrf Plots

Table 7: **Likelihood Ratio Test Results**

Model	**df**	**Italy COVID-19 Data**	**Earthquake Data**
		χ^2 (p-value)	χ^2 (p-value)
RB-TII-EHL-TL-W$(\delta, \alpha, 1, \lambda)$	1	85.9172 (< 0.001)	29.7875 (< 0.001)
RB-TII-EHL-TL-W$(\delta, 1, 1, \lambda)$	2	84.9608(< 0.001)	29.3998(< 0.001)
RB-TII-EHL-TL-W$(1, \alpha, 1, \lambda)$	2	183.0756 (< 0.001)	177.8930 (< 0.001)
RB-TII-EHL-TL-W$(1, 1, 1, \lambda)$	3	444.8533(< 0.001)	169.5852(< 0.001)

8 Conclusions

We developed a novel family of distributions called the RB-TII-EHL-TL-G distribution. We derived and established several mathematical properties of this family. A Monte Carlo simulation study was conducted using different estimation techniques, including AD, ML, CVM, AD, OLS and WLS via RMSE and Abias to assess the performance of the estimators. Based on the simulation results, it was found that ML estimation performed the best among the estimation methods considered. Consequently, it was employed to estimate the model parameters. We used two datasets to demonstrate the dominance of the new distribution over nested and several non-nested models. The results demonstrate that our newly developed model exhibit superior performance in terms of model fit and accuracy. We recommend that future researchers undertake a comparative analysis between Bayesian estimation methods and frequentist estimation techniques. This would provide valuable insights into the strengths and limitations of different estimation approaches and contribute to a deeper understanding of the RB-

TII-EHL-TL-G family of distributions and its applications.

Funding Statement

This research did not receive any sponsorship from individuals or organizations.

Declaration of competing interest

The authors assert that there are no conflicts of interest among them.

Acknowledgement

The authors express their profound gratitude to the Editor of the journal and the anonymous referees for their invaluable contributions in reviewing and enhancing the quality of this manuscript.

The Appendix of this paper is found at:
https://drive.google.com/file/d/1tQnEyGo-5JnbGGFmaQHRiC5HpK-fzJzp/view?usp=sharing

References

Ali, S., Dey, S., Tahir, M., and Mansoor, M. (2021). The Poisson Nadarajah-Haghighi distribution: different methods of estimation. *Journal of Reliability and Statistical Studies*, 14(2):415–450.

Almetwally, E. M., Abdo, D. A., Hafez, E., Jawa, T. M., Sayed-Ahmed, N., and Almongy, H. M. (2022). The new discrete distribution with application to covid-19 data. *Results in Physics*, 32(2022).

Alsultan, R. (2023). The Marshall-Olkin Pranav distribution: theory and applications. *Pakistan Journal of Statistics and Operation Research*, 19(1):155–166.

Anderson, T. W. and Darling, D. A. (1952). Asymptotic theory of certain" goodness of fit" criteria based on stochastic processes. *The Annals of Mathematical Statistics*, 23(2):193–212.

Chamunorwa, S., Oluyede, B., Makubate, B., and Chipepa, F. (2021). The exponentiated odd Weibull-Topp-leone-G family of distributions: model, properties and applications. *Pakistan Journal of Statistics*, 37(2):143–158.

Chipepa, F., Oluyede, B., Makubate, B., et al. (2020). The Topp-Leone-Marshall-Olkin-G family of distributions with applications. *International Journal of Statistics and Probability*, 9(4):15–32.

Dey, S., Ali, S., and Park, C. (2015). Weighted exponential distribution: properties and different methods of estimation. *Journal of Statistical Computation and Simulation*, 85(18):3641–3661.

Gabanakgosi, M., Moakofi, T., Oluyede, B., and Makubate, B. (2021). The gamma odd power generalized Weibull-G family of distributions with applications. *Journal of Statistical Modelling: Theory and Applications*, 2(2):79–101.

Macdonald, P. (1971). Estimation procedure for mixtures of distributions. *Journal of The Royal Statistical Society Series B-Statistical Methodology*, 33(2):102–107.

Moakofi, T., Oluyede, B., and Chipepa, F. (2021). Type II exponentiated half-logistic-Topp-Leone-G power series class of distributions with applications. *Pakistan Journal of Statistics and Operation Research*, 17(4):885–909.

Oluyede, B., Chipepa, F., and Wanduku, D. (2021). The odd Weibull-Topp-Leone-G power series family of distributions: model, properties and applications. *Journal of Nonlinear Sciences and Applications*, 14(2021):268–286.

Oluyede, B., Dingalo, N., and Chipepa, F. (2023). The Topp-Leone-Harris-G family of distributions with applications. *International Journal of Mathematics in Operational Research*, 24(4):554–582.

Oluyede, B. and Moakofi, T. (2022). Type II exponentiated half-logistic-Gompertz Topp-Leone-G family of distributions with applications. *Central European Journal of Economic Modelling and Econometrics*, 14(4):415–461.

Oluyede, B. and Moakofi, T. (2023). The gamma-Topp-Leone-Type II-exponentiated half logistic-G family of distributions with applications. *Stats*, 6(2):706–733.

Oluyede, B., Moakofi, T., and Chipepa, F. (2022a). The odd power generalized Weibull-G power series class of distributions: properties and applications. *Statistics in Transition new series*, 23(1):89–108.

Oluyede, B., Peter, P. O., Ndwapi, N., and Bindele, H. (2022b). The exponentiated half-logistic odd Burr III-G: model, properties and applications. *Pakistan Journal of Statistics and Operation Research*, 18(1):33–57.

Oluyede, B. O., Makubate, B., Wanduku, D., Elbatal, I., and Sherina, V. (2017). The gamma-generalized inverse Weibull distribution with applications to pricing and lifetime data. *Journal of Computations and Modelling*, 7(2):1–28.

Peter, P. O., Oluyede, B., Bindele, H. F., Ndwapi, N., and Mabikwa, O. (2021). The gamma odd Burr III-G family of distributions: model, properties and applications. *Revista Colombiana de Estadística*, 44(2):331–368.

Rényi, A. (1961). On measures of entropy and information. In *Proceedings of the Fourth Berkeley Symposium on Mathematical Statistics and Probability*, volume 4, pages 547–562.

Ristić, M. M. and Balakrishnan, N. (2012). The gamma-exponentiated exponential distribution. *Journal of statistical computation and simulation*, 82(8):1191–1206.

Shaked, M. and Shanthikumar, J. (2007). Stochastic orders and their applications.

Swain, J. J., Venkatraman, S., and Wilson, J. R. (1988). Least-squares estimation of distribution functions in Johnson's translation system. *Journal of Statistical Computation and Simulation*, 29(4):271–297.

Topp, C. W. and Leone, F. C. (1955). A family of J-shaped frequency functions. *Journal of the American Statistical Association*, 50(269):209–219.

Warahena-Liyanage, G., Oluyede, B., Moakofi, T., and Sengweni, W. (2023). The new exponentiated half logistic-Harris-G family of distributions with actuarial measures and applications. *Stats*, 6(3):773–801.